



UMEÅ UNIVERSITY

New Light on Photoprotection

Spectral Resolution of Non-Photochemical Quenching

Sanchali Nanda

Umeå Plant Science Centre
Department of Plant Physiology
Umeå University, Umeå, Sweden, 2025

This work is protected by the Swedish Copyright Legislation (Act 1960:729)

Dissertation for PhD

ISBN: 978-91-8070-583-7 (print)

ISBN: 978-91-8070-584-4 (pdf)

The front cover features a chloroplast electron micrograph and chlorophyll fluorescence spectra; the back cover showcases a sketch by Varvara Dikaya

Electronic version available at: <http://umu.diva-portal.org/>

Printed by: Tryckservice at Umeå University

Umeå, Sweden 2025

To Maa & Baba

Contents

Abstract	6
Abbreviations	7
Sammanfattning på Svenska	9
Popular Science Summary	10
List of Manuscripts	11
Introduction	12
1. Photosynthesis and its Regulation	12
1.1 The Organelle in Focus: Chloroplast	12
1.2 Photosynthesis: From Light Harvesting to Carbon Metabolism	13
1.3 Photoprotection	16
2. Non-Photochemical Quenching (NPQ)	18
2.1 Mechanisms of Photoprotection by NPQ	19
3. Chlorophyll Fluorescence as a Proxy for NPQ	23
3.1 A Historical Perspective	23
3.2 Chlorophyll Fluorescence	23
4. Probing Non-Photochemical Quenching of Chlorophyll Fluorescence	26
5. Spectral Decomposition and Analysis Techniques for Chlorophyll Fluorescence	28
5.1 Curve Fitting of Chlorophyll Fluorescence Spectra	28
5.2. Global Target Analysis	29
5.3. Multivariate Curve Resolution - Alternating Least Squares (MCR-ALS)	30
5.4. Comparison of Global Target Analysis and MCR-ALS	30
6. Thylakoid Organisation and Response to Light	32
7. The Elusive Role of PsbS and its Relationship with Zeaxanthin	33
7.1 Homology of PsbS, VDE and ZEP in <i>Arabidopsis</i> and <i>Populus</i>	34
8. Natural Variation in Photosynthesis Traits - Population Level Studies	36

Aims and Objectives of the Thesis	38
Results and Discussion	39
1. Development of Parameters and Analytical Methods for Chlorophyll Fluorescence Data from ChloroSpec	39
1.1. A Typical Measuring Sequence	39
1.2. Wavelength-Dependent FI' Curves and NPQ Measurements	40
1.3 Spectro-Kinetic Analysis of Chlorophyll Fluorescence Data	44
2. Insights into PSII and PSI contribution to NPQ: Spectroscopic Characterisation and its Correlation with Thylakoid Ultrastructure	
2.1. MCR-ALS Spectro-Kinetic Analysis of <i>Arabidopsis</i> , Aspen and Pine	48
2.2. Role of PsbS and Zeaxanthin in Spillover Complex Formation	51
2.3. Light-Induced Thylakoid Reorganisation and Its Impact on Quenching	55
3. Exploring Photosynthetic Variation and Genetic Adaptations in Swedish Aspen	61
4. Uncovering Molecular Players of the qH Photoprotective Mechanism in <i>Arabidopsis thaliana</i>	64
Conclusions & Perspectives	65
Acknowledgements	69
References	71

Abstract

This thesis investigates non-photochemical quenching (NPQ), emphasizing molecular mechanisms, thylakoid organisation and photosynthetic variability in plants. Spectro-kinetic analysis using ChloroSpec enabled detection of direct energy transfer from photosystem II (PSII) to photosystem I (PSI) - “spillover” - and the dissection of a unified NPQ mechanism, revealing photosystem II subunit S (PsbS) and zeaxanthin as critical regulators. PsbS facilitates light harvesting complex II (LHCII) quenching and spillover, while zeaxanthin accelerates spillover formation, ensuring rapid energy dissipation. The absence of these components severely affected the occurrence of spillover, underscoring their synergistic roles in photoprotection. Hybrid aspen mutants highlighted conserved functions of PsbS and zeaxanthin in angiosperms, with plant species-specific differences in NPQ kinetics. Aspen exhibited faster spillover occurrence and superior spillover characteristics compared to *Arabidopsis*, reflecting its enhanced photoprotective capacity. Transmission electron microscopy (TEM) linked NPQ to changes in thylakoid ultrastructure. Light-induced NPQ decreased grana layers per stack and increased stack numbers in wild-type *Arabidopsis*. Zeaxanthin levels affected the trends in thylakoid reorganisation. The Swedish aspen collection (SwAsp) study explored photosynthetic variation between genotypes and across latitudes, showing limited geographic influence but robust photoprotection via rapid NPQ induction and relaxation processes. These findings provide mechanistic insights into NPQ, its evolutionary conservation and genetic underpinnings, with implications for enhancing photosynthetic efficiency in plants under light stress.

Abbreviations

AL - actinic light-adapted state

ATP - adenosine triphosphate

CBB – Calvin-Benson-Bassham

D - dark-adapted state

ETC - electron transport chain

FI/FI' - fluorescence induction

FIR' - fluorescence induction recovery

F_m - maximal fluorescence when all PSII reaction centres are closed

F_0 - minimal fluorescence when all PSII reaction centres are open

F_v/F_m - maximum quantum efficiency of PSII

GWAS - genome-wide association studies

LED - light-emitting diode

LHC - light harvesting complex

Lhc - light harvesting chlorophyll a/b-binding

MCR-ALS - multivariate curve resolution-alternating least squares

MTF - multi-turnover flash

NADP⁺ - nicotinamide adenine dinucleotide phosphate.

NADPH - reduced nicotinamide adenine dinucleotide phosphate

NPQ - non-photochemical quenching

NPQi - non-photochemical quenching induction

NPQr - non-photochemical quenching relaxation

oePsbS - overexpression of PsbS

PC - plastocyanin

PQ - plastoquinone

PSI - photosystem I

PSII - photosystem II

PsbS - photosystem II subunit S

qE - energy-dependent quenching

qH - sustained quenching before photoinhibition

SAES - species-associated emission spectra

SNP - single nucleotide polymorphism

STF - single-turnover flash

SwAsp - Swedish aspen collection

TEM - transmission electron microscopy

VDE - violaxanthin de-epoxidase

WT - wild type

ZEP - zeaxanthin epoxidase

Sammanfattning på Svenska

Växter har en paradoxal relation till ljus. Solsken är livsviktigt för fotosyntesen, processen som upprätthåller livet på jorden, men för mycket ljus kan vara farligt. Eftersom växter inte kan flytta sig till skugga måste de förlita sig på sofistikerade molekylära skyddsmekanismer. En av dessa mekanismer, "non-photochemical quenching" (NPQ, en svensk term saknas) är av avgörande betydelse. NPQ är en sorts "överloppsskydd" gör det möjligt för växter att avleda överskottsenergi från ljus som värme, vilket skyddar fotosyntesmaskineriet från skador. Denna avhandling visar hur två nyckelmolekyler, PsbS och Zeaxantin, fungerar som "grindvakter" för NPQ och påvisar den länge debatterade mekanismen för "spillover" mellan fotosystemen i tylakoidmembranet. PsbS möjliggör "energi bortspilling" via komplex av LHC ("light harvesting chlorophyll a/b-binding" proteiner), medan Zeaxantin påskyndar bildandet av "spillover-komplex", där energi säkert överförs mellan fotosyntetiska system. Utan dessa molekyler har växter svårt att skydda sig från för mycket ljus. Avancerad elektronmikroskopi visar vidare hur NPQ omorganiserar strukturen av växternas kloroplaster vilket påverkar denna skyddsförmåga. Hybridaspår uppvisar, i jämförelse med de mest studerade arten *Arabidopsis*, snabbare NPQ-responser och ett mer effektivt skydd. Detta återspeglar antagligen trädens unika anpassningar till dynamiska ljusmiljöer, såsom det fläckvisa solljuset i skogar. En studie av naturlig variation i svenska aspträd (SwAsp) fann att deras fotosyntetesegenskaper som NPQ varierar mycket mellan olika genotyper, fast inte beroende av vilken breddgrad asparna kommer från. Genom att öka förståelsen av NPQ-mekanismerna ger denna forskning insikter som i förlängningen kan bidra till att förbättra grödors motståndskraft mot stress och jordbrukssystem bättre rustade att stärka den globala livsmedelssäkerheten.

Popular Science Summary

Plants have a paradoxical relationship with light. While sunlight is essential for photosynthesis, the process that sustains life on Earth, excessive light can be toxic. Unable to move to shade, plants must rely on sophisticated molecular mechanisms to protect themselves. Among these, non-photochemical quenching (NPQ) is vital, enabling plants to dissipate excess light energy as heat and safeguard their photosynthetic machinery from damage. This thesis reveals how two key molecules, photosystem II subunit S (PsbS) and zeaxanthin, function as "gatekeepers" of NPQ, shedding light on the long-debated mechanism of spillover between photosystems located within the thylakoid membrane. PsbS enables energy dissipation via light harvesting complexes, while zeaxanthin speeds up the formation of spillover where energy is safely transferred between photosynthetic systems. Without these molecules, plants struggle to protect themselves from excess light. Advanced imaging revealed how NPQ rearranges the chloroplast structure in plants, further enhancing its protective abilities. Hybrid aspen trees, compared to the commonly studied *Arabidopsis* plants, show faster NPQ responses and more efficient protection. This reflects the unique adaptations of trees to dynamic light environments, such as the dappled sunlight of forests. A study of natural variation in Swedish aspen trees (SwAsp) found that photosynthetic parameters like NPQ are remarkably variable between genotypes but consistent across latitudes. By shedding light on NPQ mechanisms, this research offers insights that could enhance resilience of plants to light stress, paving the way for better equipped agricultural systems to support global food security.

List of Manuscripts

Within the scope of this thesis:

Paper I

Nanda, S., Shutova, T., Cainzos, M., Hu, C., Sasbrink, B., Bag, P., Blanken, T. den, Buijs, R., Gracht, L. van der, Hendriks, F., Lambrev, P., Limburg, R., Mascoli, V., Nawrocki, W.J., Reus, M., Parmessar, R., Singerling, B., Stokkum, I.H.M., Jansson, S. and Holzwarth, A.R. (2024) **‘ChloroSpec: A new in vivo chlorophyll fluorescence spectrometer for simultaneous wavelength- and time-resolved detection’**, *Physiologia Plantarum*, 176(2), p. e14306. Available at: <https://doi.org/10.1111/ppl.14306>

Paper II

Nanda, S., Cainzos, M., Shutova, T., Fataftah, N., Fleig, V., Lihavainen-Bag, J., Bag, P., Holzwarth, A.R. and Jansson, S. (2025) **‘Spillover is the dominant non-photochemical quenching mechanism in angiosperms’**, *bioRxiv*, p. 2025.01.26.634902. Available at: <https://doi.org/10.1101/2025.01.26.634902>

Paper III

Nanda, S., Robinson K., Cainzos, M. and Jansson S **‘Natural variation in chlorophyll fluorescence traits in the Swedish aspen collection’** (Manuscript)

Paper IV

Bru, P., **Nanda, S.** and Malnoë, A. (2020) **‘A genetic screen to identify new molecular players involved in photoprotection qH in *Arabidopsis thaliana*’**, *Plants*, 9(11), p. 1565. Available at: <https://doi.org/10.3390/plants9111565>

Beyond the scope of this thesis:

Bag, P., Shutova, T., Shevela, D., Lihavainen, J., **Nanda, S.**, Ivanov, A.G., Messinger, J. and Jansson, S. (2023) **‘Flavodiiron-mediated O₂ photoreduction at photosystem I acceptor-side provides photoprotection to conifer thylakoids in early spring’**, *Nature Communications*, 14(1), p. 3210. Available at: <https://doi.org/10.1038/s41467-023-38938-z>

Introduction

1. Photosynthesis and its Regulation

1.1 The Organelle in Focus: Chloroplast

Chloroplasts are the site of photosynthesis in eukaryotic phototrophic organisms including plants. It is considered a semi-autonomous organelle because it comprises a pool of deoxyribonucleic acid (DNA) coding for proteins. It is bound by a double layered membrane which encloses the thylakoid (Fig. 1). An aqueous fluid present within the inner membrane but outside the thylakoid space is termed as the stroma. Thylakoid membranes are arranged in the form of stacks known as grana. Stroma lamellae connect and separate the grana. Each thylakoid contains a set of pigment-binding proteins which are required for light absorption to drive photosynthesis. The lumen is the space enclosed by thylakoid membranes.

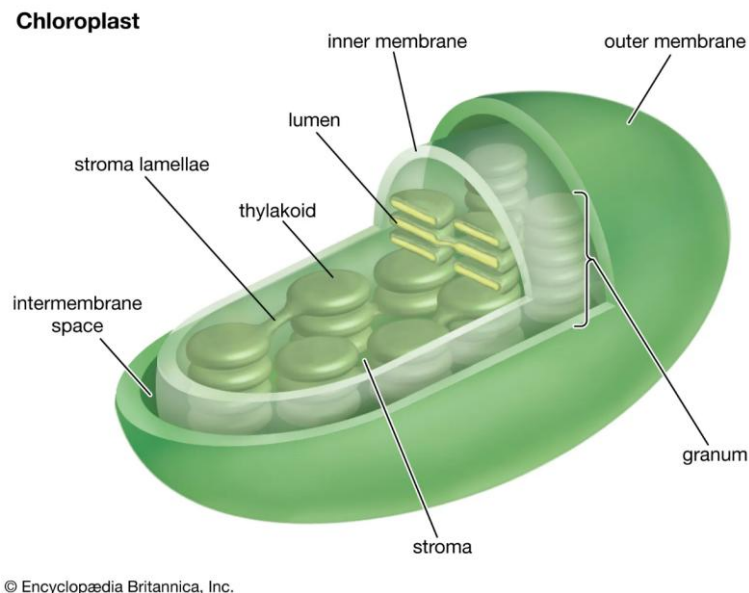


Fig. 1 Structure of a typical chloroplast in vascular plants with diameter ranging between 5-7 μm . Source: Britannica Encyclopaedia (<https://www.britannica.com/science/chloroplast#/media/1/113761/45552>)

photosystems I and II (PSI and PSII). Chlorophyll a, the primary pigment, absorbs blue and red light effectively, with absorption maxima around 428–432 nm and 660–665 nm, respectively, while chlorophyll b extends the absorption range, with maximum absorption around 452–469 nm in the blue and 642–652 nm in the red region. Carotenoids, accessory pigments like β -carotene, anthocyanins, and xanthophylls, absorb in the blue-green region (400–500 nm) (Lichtenthaler and Buschmann, 2001).

Together, these pigments absorb light in the 400–700 nm range, the photosynthetically active radiation (PAR) region of the solar spectrum. PSII and PSI each have distinct absorption characteristics, with PSI extending its absorption further into the far-red spectrum. The reaction centre pigments in PSII and PSI have peak absorption at approximately 680 nm (P680) and 700 nm (P700), respectively. This diverse pigment array optimizes energy capture, funnelling it toward PSII and PSI to initiate electron transfer.

1.2.2. Photosystem II (PSII) and Water Splitting

PSII is a key component in photosynthesis, composed of a reaction centre core and surrounding light-harvesting complexes. The reaction centre core is constituted by proteins including but not limited to CP47, CP43, D1 and D2, along with pigments like chlorophyll a, β -carotene and pheophytin a (Douady, Rousseau and Berkaloff, 1993). Light energy is funnelled to the reaction centre by the surrounding major and minor antenna complexes, which include LHClI trimers and the CP26, CP29 and CP24 proteins. The major distal antenna proteins - Lhcb1, Lhcb2 and Lhcb3 - contribute to light harvesting by forming homotrimers of Lhcb1 or heterotrimers of Lhcb1/2 and Lhcb1/3 (Jansson, 1994, 1999). These trimers are categorized as strongly (S), moderately (M), or loosely (L) bound, indicating specific binding sites around the PSII core. Recent cryo-EM studies on *Arabidopsis thaliana* reveal the detailed structure of the $C_2S_2M_2$ supercomplex at a 5.3 Å resolution, identifying precise chlorophyll positions within both core and antenna complexes (van Bezouwen *et al.*, 2017). Located in the thylakoid membrane, PSII absorbs photons through its light harvesting complex, exciting electrons and transferring them to the electron transport chain (ETC). This electron loss is balanced by splitting water molecules—a process driven by the oxygen-evolving complex (OEC), a manganese-containing cluster in PSII. The OEC extracts electrons from water, producing oxygen as a by-product and releasing protons into the thylakoid lumen, contributing

to the proton gradient used for ATP synthesis. This splitting of water is unique to PSII and essential for sustaining life, as it generates atmospheric oxygen and supplies electrons that flow through the ETC.

1.2.3. Electron Transport Chain (ETC) and ATP Synthesis

Once light energy excites electrons in PSII, the electrons enter the ETC, a sequence of protein complexes and mobile carriers within the thylakoid membrane. From PSII, electrons are transferred to plastoquinone (PQ), which shuttles them to the cytochrome b_6/f complex. This complex pumps protons into the thylakoid lumen, establishing a proton gradient critical for ATP production, and then passes the electrons to plastocyanin (PC), a mobile carrier. The proton gradient generated across the thylakoid membrane drives ATP synthase, an enzyme that synthesizes ATP from ADP and inorganic phosphate. ATP synthesis, fuelled by this gradient, provides energy for the CBB cycle. Electrons continue from PC to PSI, where they will be used to produce NADPH, linking the light-dependent reactions with carbon fixation in the next stages of photosynthesis.

1.2.4. Photosystem I (PSI) and NADPH Formation

PSI is a highly efficient photochemical complex that drives the final electron excitation and reduction of NADP^+ to NADPH in the electron transport chain. PSI is composed of a reaction centre core (PsaA & PsaB) and specialized Lhcs in a large supercomplex structure that optimizes light capture and electron transfer. The PSI complex in plants is constituted by 156 chlorophyll molecules, 32 carotenes, 2 phylloquinones, and 3 iron-sulphur clusters (Amunts, Drory and Nelson, 2007; Mazor, Borovikova and Nelson, 2015). Light absorption in PSI is further enhanced by four peripheral antenna complexes - Lhca1, Lhca2, Lhca3, and Lhca4 - arranged symmetrically around the core as two heterodimers (Lhca1/4 and Lhca2/3) (Qin *et al.*, 2015). The Lhca antenna system contains an additional 52 chlorophyll a, 9 chlorophyll b, and 10 carotenoid molecules (Mazor, Borovikova and Nelson, 2015). Electrons transferred to PSI via plastocyanin are re-energized by absorbed photons, allowing PSI to transfer electrons through its iron-sulfur clusters and reduce NADP^+ to NADPH, essential for the CBB cycle. Direct light excitation of PSI can also independently initiate electron flow, contributing to an efficient energy transfer system in photosynthesis.

1.3 Photoprotection

In PSII, balancing absorbed light energy with its use in photosynthesis is essential, particularly under high light conditions, to prevent potential damage. At low light levels, energy absorption matches the demands of photosynthesis. However, as light intensity increases, photosynthesis reaches saturation while energy absorption remains steady, leading to excess energy (Fig. 3). This surplus can disrupt PSII function, promoting the formation of reactive oxygen species (ROS) such as hydroxyl radicals ($\cdot\text{OH}$), hydrogen peroxide (H_2O_2) and superoxide radicals (O_2^-)¹⁸. To counter this, plants and photosynthetic organisms have developed protective mechanisms known as photoprotection, which manage and dissipate excess energy. One key approach involves ROS detoxification, where carotenoids and antioxidants act as scavengers to neutralize these molecules. Another effective mechanism is to reroute surplus photon energy away from the photosynthetic apparatus, releasing it as chlorophyll fluorescence or heat. This dissipation process, termed non-photochemical quenching (NPQ), allows the system to handle excess energy by converting it to heat. NPQ is central to photoprotection,

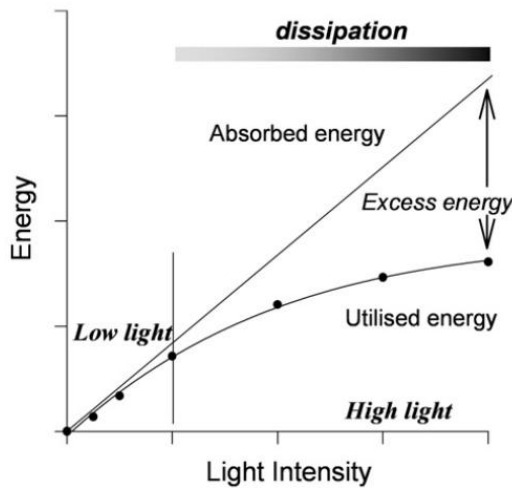


Fig. 3 With increasing light intensity, photochemistry becomes saturated, leaving the additional absorbed energy to overexcite the photosynthetic machinery. This overexcitation triggers the need for photoprotective mechanisms to prevent potential photo-oxidative damage to the system. Source: Ruban, Johnson and Duffy, 2012.

helping mitigate stress caused by high light exposure and preserving PSII functionality.

However, NPQ can be inefficient in fluctuating light conditions. In wild-type (WT) plants, NPQ does not always activate or deactivate quickly enough to match sudden changes in light, leaving the photosynthetic apparatus intermittently unprotected or in an overprotective state that limits photosynthetic efficiency. Genetically modified plants with enhanced NPQ responsiveness have been shown to better track light fluctuations, safeguarding the photosynthetic machinery and improving overall efficiency (Kromdijk *et al.*, 2016; De Souza *et al.*, 2022). Fine-tuning photoprotective systems like NPQ has promising implications for improving crop yield, an essential factor for global food security.

2. Non-Photochemical Quenching

Non-photochemical quenching (NPQ) stands as one of three primary fates for the energy absorbed by chlorophylls, alongside photochemistry and fluorescence emission (Fig. 5). Consequently, NPQ mechanisms encompass pathways that dissipate excess excitation energy as heat, providing a crucial photoprotective function against photodamage, particularly under high-light conditions. While the concepts of qE, qT, qI and spillover have shaped our understanding of NPQ since the 1990s (Krause and Weis, 1991), recent research has introduced new mechanisms and clarified existing ones through advanced experiments and mutant studies (Malnoë, 2018; Pinnola and Bassi, 2018).

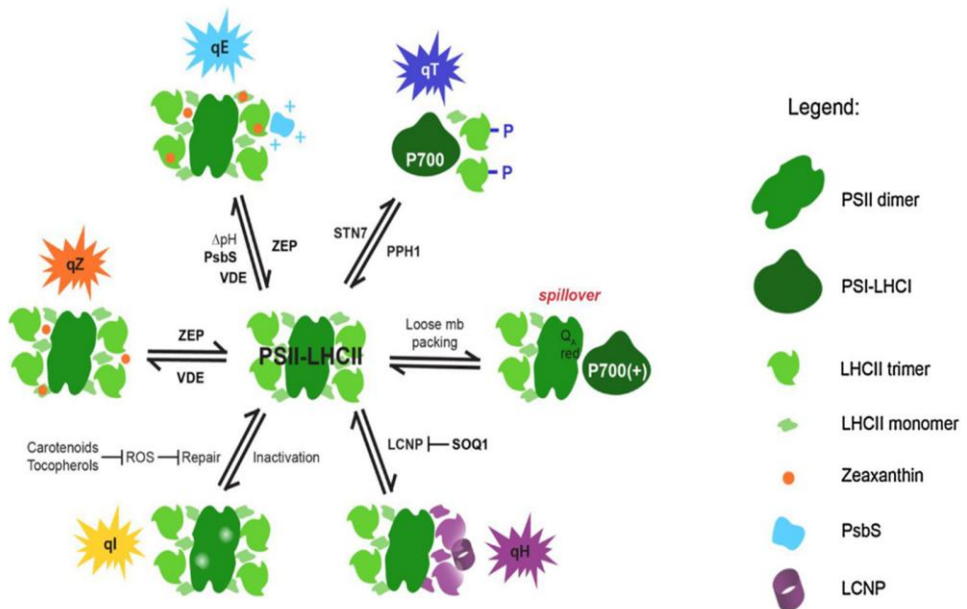


Fig. 4 Mechanisms involved in non-photochemical quenching (NPQ) in plants. Source: Malnoë, 2018.

2.1 Mechanisms of Photoprotection by NPQ

This section provides a concise examination of NPQ mechanisms, with special emphasis on PSII-PSI spillover, describing them based on their molecular components and distinct modes of action (Fig. 4).

2.1.1 Spillover (PSII-PSI energy transfer)

The concept of "spillover" in photosynthesis describes the transfer of excitation energy from PSII to PSI, a mechanism that prevents overexcitation of PSII under varied light conditions, especially when PSII reaction centres are closed. First identified by Satoh and Butler in spinach (Satoh, Strasser and Butler, 1976), greater energy transfer between the photosystems was reported when PSII reaction centres were closed. Studies on *Arabidopsis thaliana* identified PSI-LHCII and PSII-LHCII supercomplexes, providing a foundation for examining spillover (Järvi *et al.*, 2011). In red algae, enhanced spillover facilitated by phycobilisomes balanced excitation energy between PSI and PSII (Yokono, Murakami and Akimoto, 2011). In lichens, spillover during desiccation protected both photosystems (Slavov, Reus and Holzwarth, 2013). In *Symbiodinium* under thermal stress, spillover dissipated excess energy to protect against coral bleaching (Slavov *et al.*, 2016). In contrast, diatoms displayed structural adaptations reducing spillover and thereby optimizing light utilisation in high-light conditions (Flori *et al.*, 2017).

More recently, the photoprotective role of PSI deep-trap chlorophylls in *Arabidopsis* and *Spinacia oleracea*, has been identified to facilitate energy dissipation in high light (Yokono *et al.*, 2019). In *Oryza sativa* (rice), stable antenna-mediated spillover mechanisms enable energy transfer within PSI-PSII megacomplexes, again an adaptation suited to high-light environments (Kim *et al.*, 2023). In cyanobacteria, differences in spillover efficiency between intact and isolated thylakoids suggest that membrane organisation influences spillover (Akhtar *et al.*, 2024). Further, spillover becomes prominent under low light in *Spinacia oleracea* and *Alocasia odora*, contradicting assumptions that it primarily supports high-light acclimation (Terashima *et al.*, 2024). Low pH conditions stabilize PSI-PSII interactions in *Arabidopsis*, promoting spillover for photoprotection (Yokono, Noda and Minagawa, 2024). Collectively, these studies demonstrate spillover as an adaptive photoprotective mechanism across diverse photosynthetic organisms,

regulated by structural, environmental, and biochemical factors, thereby tipping the excitation energy balance from PSII to PSI.

2.1.2 qE (quenching dependent on Energy)

Predominantly known as the fastest component of NPQ, qE can be induced within seconds and relaxes in minutes in darkness. Acidification of thylakoid lumen leads to protonation of PsbS which triggers the induction of qE (Li *et al.*, 2000). A quenching site is created by PsbS in alliance with carotenoid pigment zeaxanthin by reorganisation of LHCII in the thylakoid membrane (Johnson *et al.*, 2011). Although the role of zeaxanthin in NPQ had been uncovered quite early in the field (Demmig *et al.*, 1987), the mystery behind its exact function in qE was known much later when the importance of xanthophyll cycle enzymes – violaxanthin de-epoxidase (VDE) and zeaxanthin epoxidase (ZEP) came to light (Niyogi, Bjorkman and Grossman, 1997; Niyogi, Grossman and Björkman, 1998). Fluorescence lifetime measurements revealed that while PsbS senses ΔpH and is necessary for induction of qE, VDE on the other hand is necessary for accumulation of zeaxanthin which modulates relaxation kinetics (Sylak-Glassman *et al.*, 2014). In summary, ΔpH , PsbS and zeaxanthin are the key players and are necessary for the occurrence of qE leading to thermal dissipation.

2.1.3 qI (sustained quenching by photoInhibition)

Photoinhibition is defined as the light-induced decrease in quantum yield of photosynthesis due to inactivation and/or destruction in the D1 protein of PSII. qI is a slow relaxing process, which lasts for hours or longer (Krause, 1988; Baker, 1996). Although an efficient repair machinery of PSII is in place to mend the photodamaged D1 proteins (Aro, Virgin and Andersson, 1993) when the rate of D1 damage is greater than its rate of repair, photoinhibition of PSII occurs (Takahashi and Murata, 2005). The PSII reaction centre has been revealed to be the quenching site for photoinhibition-induced energy dissipation, with quenching and damage stemming from a shared event (Nawrocki *et al.*, 2021).

2.1.4 qT (quenching by state Transitions)

Another component of NPQ was identified that is a process called state transitions and is associated with redistribution of antenna in changing light conditions (Allen *et al.*, 1981; Quick and Stitt, 1989; Allen, 2003). Over stimulation of PSII leads to phosphorylation of antenna by STN7 kinase, thus promoting its transport to PSI (state 2) enabling redistribution of energy towards PSI and preventing any damage to PSII (Bellafiore *et al.*, 2005). This mechanism is complemented by a phosphatase PPH1 which dephosphorylates the antenna and promotes transition to PSII (state 1) upon oxidation of the PQ pool (Shapiguzov *et al.*, 2010). While a decrease in fluorescence due to redistribution of energy by state transitions has been demonstrated by Nawrocki *et al.* in 2016, thermal dissipation by detached antenna is proposed by Ünlü *et al.* (Ünlü *et al.*, 2014). Interestingly, qT does not operate in saturating light conditions (Nilkens *et al.*, 2010).

2.1.5 qZ (quenching dependent on Zeaxanthin)

Accumulation of zeaxanthin is also required for a slow inducible and relaxing mechanism termed qZ, ranging from minutes to tens of minutes, leading to thermal dissipation. qZ is facilitated by the activation of VDE, which converts violaxanthin to zeaxanthin (Demmig *et al.*, 1987; Niyogi, Grossman and Björkman, 1998). Occurrence of qZ is supposed to be independent of ΔpH , PsbS and constitutes a conformational change in minor antenna protein CP26; distinguishing it from qE on a molecular basis as well (Dall'Osto, Caffarri and Bassi, 2005). NPQ kinetics analysis also revealed a zeaxanthin-dependent component, which occurred independently of qE, qT, or qI, and the term “qZ” officially came into existence (Nilkens *et al.*, 2010).

2.1.6 qM (quenching by chloroplast Movement)

Under excess light conditions, decrease in photon absorption was reported due to chloroplast avoidance movements possibly from the cell surface to the side walls of cells to decrease photodamage (Kasahara *et al.*, 2002). Further research on qE mutants led to the discovery of another quenching mechanism termed as qM which accounted for not causing thermal dissipation. qM occurs in addition to and independent of other thermal dissipation NPQ mechanisms and results in decrease of chlorophyll fluorescence (Cazzaniga *et al.*, 2013).

2.1.7 qH (sustained quenching before photoInhibition)

qH accounts for another unique slowly relaxing photoprotective quenching mechanism in the peripheral antenna of PSII leading to thermal dissipation. In 2013, Brooks et al. (Brooks *et al.*, 2013) reported that a protein SOQ1 (suppressor of quenching 1) is involved in the inhibition of a slow relaxing NPQ mechanism that works independently of other prominent NPQ components or factors such as the pH gradient, the STN7 kinase, the PsbS protein and the carotenoid pigment zeaxanthin. Later the role of LCNP (lipocalin in the plastid) as an effector protein was discovered and thus the term “qH” came into existence (Malnoë *et al.*, 2018). Another regulatory protein ROQH1 has been discovered to be involved in the relaxation of qH probably by recycling the quenching sites back to a light harvesting state (Amstutz *et al.*, 2020). More recent findings show that it operates within the major trimeric antenna complexes (LHCII) of *Arabidopsis*, where qH facilitates energy dissipation without altering pigment, lipid, or protein content (Bru *et al.*, 2022). A combination of forward genetic suppressor screen with whole-genome sequencing of *Arabidopsis* mutants has been employed to accelerate the discovery of other potential genes involved in qH (Bru, Nanda and Malnoë, 2020).

3. Chlorophyll Fluorescence as a Proxy for NPQ

3.1 A Historical Perspective

In 1874, N.J.C. Müller made the first significant observation regarding chlorophyll fluorescence by noting that a diluted chlorophyll solution fluoresced more intensely than any living green leaf. From this observation, Müller hypothesized that there was a reciprocal relationship between chlorophyll fluorescence and carbon dioxide assimilation, suggesting that when one process was active, the other would be diminished (Müller, 1874). Nearly six decades later, in 1931, Hans Kautsky and A. Hirsch made a pivotal connection between chlorophyll fluorescence and the photosynthetic process. In their seminal paper, Kautsky and Hirsch observed that when dark-adapted leaves were illuminated, the chlorophyll fluorescence initially increased rapidly and then gradually declined. This phenomenon, now known as fluorescence induction or the Kautsky effect, was the first demonstration of how fluorescence could be linked to the internal mechanisms of photosynthesis. The authors visually observed the time course of fluorescence intensity and, in a critical insight, qualitatively correlated it with the earlier work on CO₂ assimilation by Otto Warburg (Kautsky and Hirsch, 1931). This observation showed that the fluorescence rise corresponded to the saturation of the photosynthetic apparatus, particularly PSII, while the subsequent decline indicated the activation of the electron transport chain, which began utilizing the absorbed light energy for photosynthesis. H. K. Lichtenthaler reviewed the initial work by Kautsky in English (Lichtenthaler, 1992). The implications of Kautsky and Hirsch's work were far-reaching, as it laid the foundation for the development of modern fluorimetry techniques which are now used to assess photosynthetic efficiency, plant stress, and the regulation of light energy in plants.

3.2 Chlorophyll Fluorescence

Leaves in plants contain major pigments, primarily chlorophyll a and chlorophyll b, which play complementary roles in capturing light energy for photosynthesis. Chlorophyll a, the primary pigment, is responsible for capturing photons efficiently due to its conjugated double bond system, which enables electron excitation to higher energy states (Weiss, 1972). In terms of absorption, chlorophyll a absorbs light most

effectively in the 428–432 nm (blue) and 660–665 nm (red) regions, while chlorophyll b absorbs in the 452–469 nm (blue) and 642–652 nm (red) regions (Lichtenthaler and Buschmann, 2001). This complementary absorption spectrum allows chlorophyll b to act as an accessory pigment, transferring absorbed energy to chlorophyll a and thereby enhancing the overall efficiency of light capture. Once excited by light, chlorophyll a molecules can dissipate the absorbed energy in several ways: (1) by fuelling photochemical reactions, (2) by dissipating as heat via internal conversion, or (3) by emitting fluorescence, a radiative decay process as represented in Fig. 5. This chlorophyll fluorescence typically shifts to red or far-red wavelengths (680–740 nm) and represents a small fraction of the absorbed energy, providing insights into the photosynthetic efficiency and health of the plant (Govindjee and Yang, 1966). Additionally, fluorescence originates from both photosystems; however, while PSII contributes prominently, PSI fluorescence is

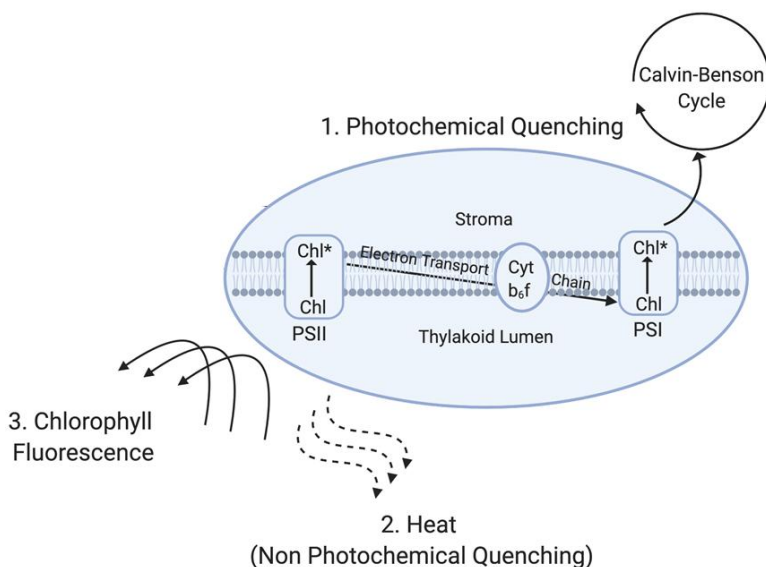


Fig. 5 Three major fates of excited chlorophyll in plants. Upon receiving sunlight, chlorophyll pigments as part of the antennae on the thylakoid membrane are excited and thereby initiate the photosynthetic electron transport chain to activate metabolic processes such as Calvin-Benson-Bassham (CBB) cycle resulting in photochemical quenching (1). The surplus excitation energy in the antenna is dissipated via heat (2); of which non photochemical quenching (NPQ) forms a major component and chlorophyll fluorescence (3). Created with BioRender.com

minimal because it remains highly quenched under typical conditions. P700, primary donor of PSI, often exists in an oxidized state, leading to more stable and subdued fluorescence compared to the dynamic response seen in PSII (Krause and Weis, 1991).

4. Probing Non-Photochemical Quenching of Chlorophyll Fluorescence

Traditional laboratory techniques for NPQ measurement involve pulse-amplitude modulation (PAM) and direct detection, both widely used in research (Genty, Briantais and Baker, 1989; Strasser and Govindjee, 1992). While these methods offer effective tools for assessing fluorescence signals, they are limited in spectral resolution, typically capturing a single, wavelength-integrated fluorescence response due to early technological constraints in light detection (Kalaji *et al.*, 2014, 2017). Although attempts have been made to split fluorescence detection into two wavelength regions, fully wavelength-resolved fluorescence detection is generally not feasible with current commercial instruments (Pfündel, 2021).

In contrast, ultrafast chlorophyll fluorescence measurements, have pushed the boundaries by offering both time and wavelength resolution, essential for distinguishing NPQ components with precision. These methods enable the separation of fluorescence components by their specific kinetic and spectral profiles (Holzwarth, Wendler and Haehnel, 1985; Holzwarth, 1986; Holzwarth *et al.*, 2009; Holzwarth and Jahns, 2014; Chukhutsina, Holzwarth and Croce, 2019; Croce and van Amerongen, 2020). However, such techniques are complex and expensive, making them less accessible for general research or field use and typically limiting their deployment to controlled laboratory conditions where specialized expertise is available.

There remains a significant gap for accessible, wavelength- and time-resolved fluorescence instruments suitable for use outside specialized labs, in settings like greenhouses or field studies. The ChloroSpec spectrometer has been developed to address this need by integrating full wavelength resolution in an easy-to-use format, combining the advantages of traditional fluorometers with enhanced spectral capabilities (Nanda *et al.*, 2024). The ChloroSpec instrument operates by exciting a photosynthetic sample with one of three light-emitting diode (LED) sources - red, green, or infrared (625 nm, 530 nm, and 730 nm) - and simultaneously capturing fluorescence emissions through two detection systems. First, three photodiode-filter combinations detect fluorescence at key wavelengths (typically 686 nm, 700 nm, and 730 nm) with high temporal resolution, capturing rapid fluorescence induction

traces. Second, a full-spectrum optical spectrometer, spanning 500-900 nm, collects a comprehensive emission profile that forms a 3D data surface of intensity vs. wavelength vs. time (Fig. 6). This full-spectrum data allows to separate fluorescence into distinct spectral components, revealing different kinetic behaviours using spectro-kinetic modelling as detailed in the Results section.

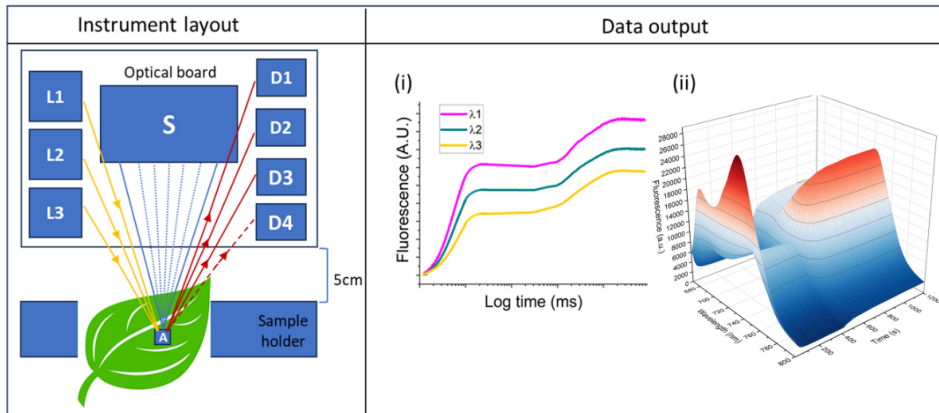


Fig. 6 Schematic representation of the working principle of ChloroSpec. A leaf sample is illuminated by one of three LED sources (red, green, or infrared: L1, L2, L3), and emitted fluorescence is detected via: (i) filter-photodiode combinations (D1 = 686 nm, D2 = 700 nm, D3 = 730 nm) and a reference photodiode (D4) for high time resolution and wavelength-specific fluorescence induction traces; and (ii) a spectrometer (500–900 nm range) for full spectral detection, generating a 3D plot of intensity vs. wavelength vs. time. The detection area on the leaf surface is 5 mm^2 ("A"). Source: Nanda *et al.*, 2024.

5. Spectral Decomposition and Analysis Techniques for Chlorophyll Fluorescence

Spectral decomposition is the process of resolving complex spectroscopic data into constituent components, enabling the extraction of individual spectral features and their temporal or spatial evolution. This approach is crucial for analysing overlapping signals in datasets obtained from techniques like fluorescence spectroscopy, where multiple processes or states contribute to the observed spectra.

5.1 Curve Fitting of Chlorophyll Fluorescence Spectra

This section introduces a method commonly used for spectral decomposition to illustrate the two fundamental principles of modelling and fitting, which form the foundation of the kinetic modelling presented in the main results of this thesis. Specifically, these principles involve (1) decomposing complex spectra into distinct components and (2) iteratively refining the model to improve its fit to the data. A typical example of curve fitting is shown in Fig. 7, where the addition of a third peak improves the cumulative fit of the spectra, demonstrating the value of these principles in capturing spectral complexity. Numerous studies support the applicability of this approach (Sugiyama and Murata, 1978; Subhash and Mohanan, 1997; Küpper, Spiller and Küpper, 2000).

We extend these principles to our kinetic model by incorporating additional spectral species to achieve better fits in analyses performed using global target analysis and multivariate curve resolution–alternating least squares (MCR-ALS), as described later in the thesis. The decomposition principle ensures that all significant spectral features are represented, while the iterative refinement principle allows us to optimize the model's accuracy. An additional advantage of using global target analysis and MCR-ALS methods lies in their ability to obtain a fit using a kinetic model over time, enabling the evaluation of overall spectral shapes across temporal data rather than decomposing individual spectra from NPQ kinetics experiments. This approach integrates the two principles into a 3D framework (time and spectra), offering a more powerful and comprehensive analysis compared to the limitations of 2D methods that analyse each spectrum separately. By combining decomposition and iterative refinement, our method captures the dynamic processes underlying NPQ more effectively.

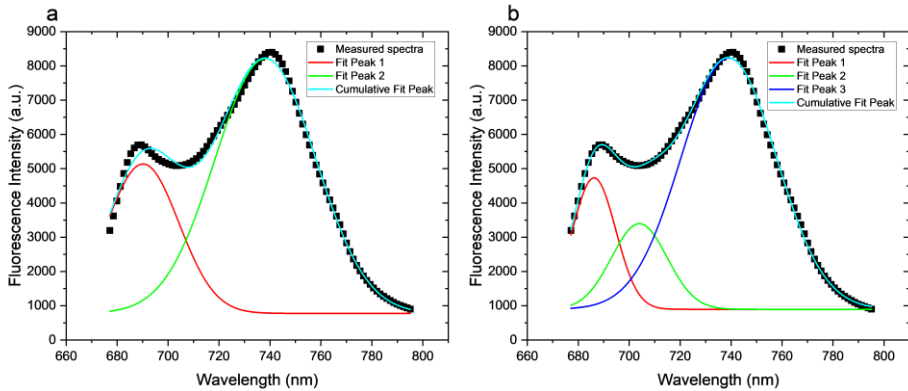


Fig. 7 An example of curve fitting of chlorophyll fluorescence spectra using the Gauss model. A cumulative model fit is obtained by choosing (a) 2 peaks and (b) 3 peaks respectively for initial estimation of the model parameters. The spectra used for fitting was obtained from a dark-adapted wild-type *A. thaliana* leaf exposed to $600 \mu\text{mol m}^{-2} \text{s}^{-1}$ red excitation light for 2 seconds.

5.2. Global Target Analysis

This is a powerful mathematical tool for interpreting spectroscopic data by fitting experimental measurements to kinetic models. It involves defining target functions based on prior knowledge or hypotheses about the system, allowing the identification of specific components and their kinetics (Fig. 8). This method is particularly effective in elucidating reaction mechanisms and is essential for integrating known biological information through a kinetic model and aligning it with experimental data (Holzwarth, 1996; van Stokkum, Larsen and van Grondelle, 2004).

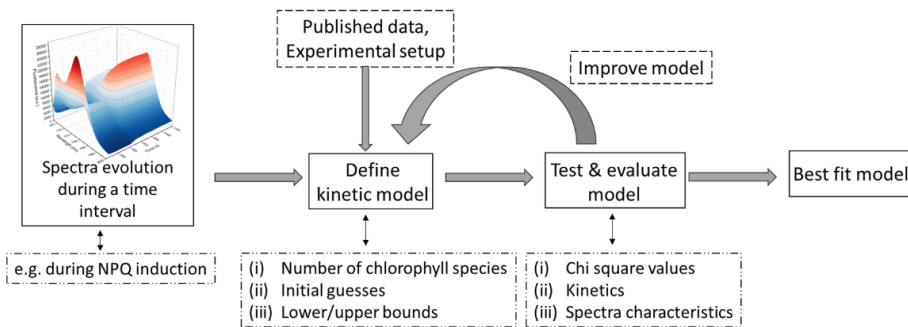


Fig. 8 Schematic workflow of global target analysis. Source: Nanda *et al.*, 2024.

5.3. Multivariate Curve Resolution – Alternating Least Squares (MCR-ALS)

This is another widely used method for spectral analysis, particularly when no prior kinetic model is available. MCR-ALS resolves spectroscopic data into pure component spectra and their associated concentration profiles by iteratively optimizing these components under constraints such as non-negativity or unimodality. This method is flexible and model-independent, making it suitable for complex systems with unknown dynamics (Rutan, de Juan and Tauler, 2020).

Together, these techniques offer complementary approaches to untangle intricate spectroscopic datasets, facilitating a deeper understanding of the underlying processes.

5.4. Comparison of Global Target Analysis and MCR-ALS

Global target analysis and MCR-ALS are powerful methods for spectral decomposition, each with distinct strengths and limitations. Global target analysis integrates experimental data with predefined kinetic models, leveraging prior biological knowledge to extract specific components and their kinetics. However, its fitting process is constrained by the parameters of the kinetic model, limiting flexibility when dynamics of the system are not fully understood. In contrast, MCR-ALS does not require a predefined model, making it more flexible for analysing systems with unknown or complex kinetics. By resolving data into pure component spectra and concentration profiles under constraints like non-negativity, MCR-ALS offers a data-driven approach. While global target analysis excels in hypothesis-driven scenarios, MCR-ALS is ideal for exploratory analyses where model independence is key. The main differences are summarised in Fig. 9.

$$D(t, \lambda) = C(t) \cdot S^T + E$$

	Global Target Analysis	MCR-ALS
Dependency	Kinetic Model	No predefined model; relies on constraints
Method for C(t)	Solved using kinetic equations	Optimized iteratively with ALS
Method for S^T	Refined based on the kinetic model	Optimized iteratively with ALS
Flexibility	Limited by model assumptions.	Highly flexible for complex systems
Assignment of Spectra	Tied to kinetic model and spectral comparisons	Uses spectral shapes and C(t) trends
Residual Error Analysis	Minimizes residual within kinetic model constraints	Includes regularization to avoid overfitting

Fig. 9 Comparison of global target analysis and MCR-ALS method for spectro-kinetic decomposition. The equation represents the decomposition of the observed data matrix $D(t, \lambda)$, where rows correspond to time points (t) and columns correspond to wavelengths (λ), into two components: $C(t)$ and S^T . The matrix $C(t)$ describes the time-dependent concentration profiles of individual components, while S^T contains the spectral signatures of these components. The transpose (S^T) aligns the dimensions of the spectral matrix S (components \times wavelengths) with $C(t)$ (time points \times components) to enable matrix multiplication, ensuring compatibility with the experimental data structure. This framework allows for the reconstruction of the observed dataset. Residual errors (E), represent noise or unexplained variance in the decomposition.

6. Thylakoid Organisation and Response to Light

Lateral heterogeneity in thylakoid membranes refers to the spatial separation of photosynthetic complexes. PSII and LHCII are concentrated in the grana stacks, where light energy is captured and initiates the water-splitting process. PSI and ATP synthase are located in the stroma lamellae, which are unstacked regions of the thylakoid. (Andersson and Anderson, 1980). This separation reduces competition between PSII and PSI for light energy and electron carriers, enabling a sequential flow of electrons from PSII to PSI, thereby increasing the efficiency of linear electron flow (Fig. 10).

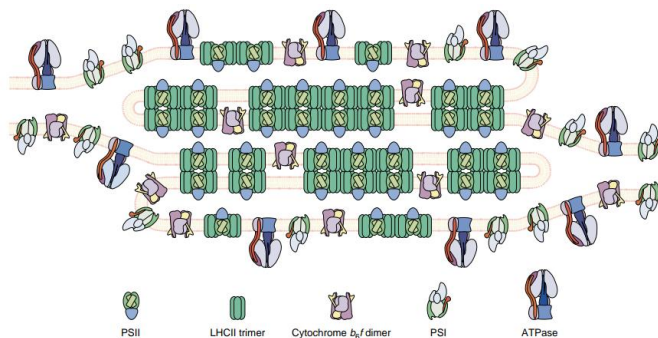


Fig. 10 Lateral heterogeneity of photosystems and protein complexes in thylakoid membranes. Source: Allen and Forsberg, 2001.

Thylakoid organisation is regulated by genetic and ionic factors that adapt to changing light conditions. Under low-light, state transitions prevail - STN7 phosphorylates LHCII, decreasing grana diameter and enabling LHCII movement between PSII and PSI, balancing excitation energy. In high-light, TAP38 dephosphorylates LHCII in high light, leading to increased grana stacking and enhancing energy dissipation via non-photochemical quenching (Wood *et al.*, 2019). CURT1 affects grana size, with overexpression creating narrow stacks with more layers and absence resulting in wider grana with fewer layers (Armbruster *et al.*, 2013). Light-induced Cl^- and Ca^{2+} influx causes lumen swelling, enhancing protein mobility, while ΔpH formation leads to larger, more stacked grana due to counterion movements (reviewed in Pribil, Labs and Leister, 2014; Johnson and Wientjes, 2020).

7. The Elusive Role of PsbS and its Relationship with Zeaxanthin

The intricate interplay between the PsbS protein and the xanthophyll pigment zeaxanthin in NPQ has been progressively unravelled through numerous studies. Initially, PsbS was identified as capable of binding zeaxanthin, which induced a significant red shift in zeaxanthin's absorption spectrum and facilitated an "activated" state necessary for energy dissipation (Aspinall-O'Dea *et al.*, 2002). Subsequent research demonstrated that PsbS alone could initiate NPQ even in the absence of zeaxanthin, suggesting that while zeaxanthin acts as an allosteric activator, PsbS can independently trigger energy dissipation (Crouchman, Ruban and Horton, 2006). Contrary to early assumptions, it was found that the dependence of NPQ on xanthophylls does not result from direct binding of lutein or zeaxanthin to PsbS. Instead, other pigment-binding proteins, likely within the Lhcb family, mediate this dependency through xanthophylls (Bonente *et al.*, 2008). Additionally, studies on *Arabidopsis* mutants revealed that plants lacking PsbS still possess a functional NPQ mechanism, albeit less efficient, indicating that PsbS enhances but is not essential for NPQ (Johnson and Ruban, 2010, 2011). Structural analyses provided deeper insights, revealing that PsbS has a unique fold and dimerisation pattern distinct from other light-harvesting complexes. Under low pH conditions, PsbS transitions from a dimer to a monomer, acting as a pH-sensitive trigger that activates NPQ to dissipate excess light energy as heat (Fan *et al.*, 2015).

Optimal NPQ requires both PsbS and zeaxanthin. PsbS influences the organisation of pigment-protein complexes, particularly LHCII, facilitating the incorporation of zeaxanthin and enhancing excitation quenching (Wilk *et al.*, 2013). Structures containing violaxanthin, by contrast, show reduced energy dissipation (Welch *et al.*, 2021). Furthermore, the interaction between PsbS and LHCII is regulated by both the transmembrane pH gradient (ΔpH) and zeaxanthin levels, promoting effective NPQ (Sacharz *et al.*, 2017). Notably, it has been elucidated that PsbS does not affect the relaxation dynamics of excited chlorophyll, a role primarily attributed to zeaxanthin (Sylak-Glassman *et al.*, 2014). PsbS-lacking mutants under sudden high light suffered more photodamage compared to zeaxanthin-lacking mutants (Ware, Belgio and Ruban, 2015). This highlights distinct, complementary roles where

PsbS primarily influences rapid quenching onset, while zeaxanthin adjusts the relaxation dynamics.

7.1 Homology of PsbS, VDE, and ZEP in *Arabidopsis* and *Populus*

Homologs of the PsbS, ZEP, and VDE proteins in hybrid aspen (*P. tremula* × *P. tremuloides*), *P. trichocarpa*, *P. tremula*, and *P. tremuloides* were analyzed based on their amino acid sequences and compared with

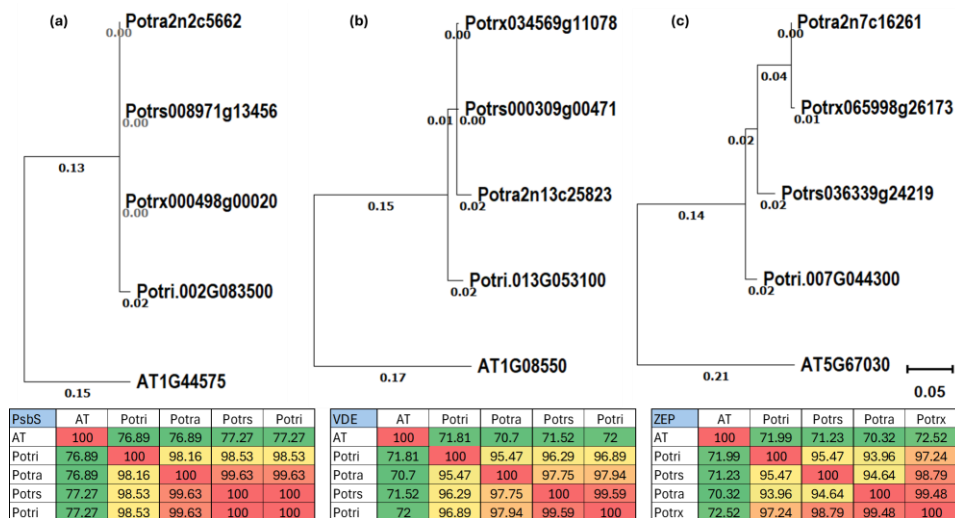


Fig. 11 Phylogenetic tree and percent identity matrix for protein sequence homology analysis for (a) PsbS, (b) VDE and (c) ZEP. The phylogenetic tree displays evolutionary relationships among selected genes, constructed using the Maximum Likelihood (ML) method in MEGA X (Kumar *et al.*, 2018). Branch lengths are scaled to represent evolutionary distance, as indicated by the scale bar. Branch length variability provides insights into the relative divergence among sequences, where shorter branches indicate higher similarity and potential functional conservation. The heatmap illustrates percent identity between each pair of genes computed by Clustal2.1 (Madeira *et al.*, 2024), color-coded from green (low percent identity) to red (high percent identity). Red hues represent higher similarity, while green hues indicate lower similarity, visually highlighting regions of sequence homology. AT is *Arabidopsis thaliana*, Potri is *Populus trichocarpa*, Potra is *Populus tremula*, Potrs is *Populus tremuloides*, Potrx is *Populus tremula* × *Populus tremuloides* (hybrid aspen). The amino acid sequences were obtained from PlantGenIE.org (Sundell *et al.*, 2015).

counterparts in *Arabidopsis thaliana*. Phylogenetic analysis of these protein sequences reveals a close evolutionary relationship between *Arabidopsis* and *Populus*, with evolutionary distances ranging from 0.02 to 0.07 substitutions per site. The *Populus* proteins exhibit even higher conservation within the genus, with distances between 0 to 0.02 substitutions per site. The percent identity matrix corroborates these findings, showing 70-77% amino acid sequence similarity between *Arabidopsis* and *Populus* (Fig. 11).

8. Natural Variation in Photosynthesis Traits - Population Level Studies

Leveraging the natural genetic diversity in photosynthesis-related traits presents substantial opportunities for improving plant yields and resilience. Recent studies underscore that natural variation within photosynthetic traits can significantly influence plant productivity, particularly in wheat, where enhancing photosynthesis in key tissues has been linked to improved yield through greater grain numbers and weight (Faralli and Lawson, 2020). This diversity is shaped by evolutionary pressures as plants adapt to various environments, creating genetic pools that could be harnessed in breeding for photosynthetic efficiency and productivity.

Mapping techniques like genome-wide association studies (GWAS) have advanced our understanding of these traits by identifying associated genes. Initially popularized in *Arabidopsis thaliana* due to its available genomic resources, GWAS has become essential for exploring genetic factors in crops, extending to studies of traits in rice and wheat, among others (Atwell *et al.*, 2010; Huang *et al.*, 2010; Driever *et al.*, 2014). The effectiveness of GWAS in identifying key genes largely depends on several factors, including the genetic architecture of traits, which are more easily dissected when governed by a few genes with significant phenotypic effects. Environmental conditions and population structures are also crucial; for instance, GWAS analysis of salt-tolerance markers in rice showed that the association of candidate genes varied with salt treatment duration (Patishtan *et al.*, 2018). In maize, high-throughput phenotyping in controlled environments was shown to enhance the accuracy of predictive models, underscoring the importance of environmental consistency in phenotype scoring (Wang *et al.*, 2023).

As crop studies continue to develop, non-domesticated plant populations present complementary genetic resources due to their typically higher genetic diversity. For instance, the Swedish aspen (SwAsp) collection has provided valuable insights into aspen (*Populus tremula*) genetics, where GWAS identified the *PtFT2* gene as a major contributor to bud set variation, strongly associated with latitude (Wang *et al.*, 2018). Other studies on the SwAsp population have explored associations with wood traits and growth, though not all have yielded significant loci (Grimberg *et al.*, 2018; Mähler *et al.*, 2020).

Photosynthetic traits often link to regulatory rather than structural genes, likely due to the evolutionary conservation of core photosynthetic components, with selection pressures influencing regulation over time. High-throughput chlorophyll fluorescence techniques have proven particularly valuable in photosynthetic research, as they non-invasively assess PSII efficiency and stress responses (Rungrat *et al.*, 2016; Tsai *et al.*, 2019; Ferguson *et al.*, 2023; Feyissa *et al.*, 2024).

Aims and Objectives of the Thesis

This thesis aims to bridge critical gaps in understanding NPQ by:

1. Addressing the NPQ Mechanism: While several molecular players in NPQ have been identified, a unifying mechanism to explain this process remains elusive. To tackle this, spectral evolution of chlorophyll fluorescence throughout NPQ induction at room temperature was characterised using ChloroSpec - a new chlorophyll fluorescence spectrometer. By studying *Arabidopsis* mutants deficient in PsbS and zeaxanthin respectively, fluorescence dynamics over time were captured, offering insights that could contribute to a cohesive model of NPQ (Papers I & II).

2. Examining Functional Conservation of PsbS and Zeaxanthin in Angiosperms: As a step towards understanding whether PsbS and zeaxanthin play similar roles in NPQ in the angiosperm lineage, hybrid aspen mutants deficient in these components were generated. Functional characterisation of NPQ in these mutants allowed us to assess the evolutionary conservation of NPQ mechanisms in a tree species, broadening our insights beyond *Arabidopsis* (Paper II).

3. Linking NPQ to Thylakoid Organisation: The subsequent goal was to correlate NPQ with changes in sub-cellular organisation at the chloroplast level. Using transmission electron microscopy (TEM) followed by image analysis, alterations in thylakoid arrangements as a direct result of NPQ induction were examined. This analysis provided a structural perspective on NPQ, establishing a connection between chlorophyll fluorescence quenching and thylakoid rearrangements (Paper II).

4. Exploring Photosynthetic Variation in Aspen: To further investigate photosynthetic traits in trees, natural variation in a Swedish aspen population was studied. By utilising ChloroSpec's wavelength- and time-resolved fluorescence data, phenotypic resolution for GWAS was enhanced. This approach aimed to refine the identification of genetic loci influencing photosynthetic performance, making it possible to dissect genetic contributions to photosynthesis (Paper III).

Results and Discussion

1. Development of Parameters and Analytical Methods for Chlorophyll Fluorescence Data from ChloroSpec

ChloroSpec enabled detailed *in vivo* measurements of chlorophyll fluorescence, capturing both spectral- and time-resolved information at room temperature. By using single-turnover flash (STF) bursts to measure fluorescence induction (FI), key variations in quantum efficiency of PSII were revealed that were previously not detectable with conventional fluorescence instruments. FI' spectra, combined with spectro-kinetic analysis, allowed for the resolution of NPQ mechanisms. The following sections outline the specific parameters determined in the experiments, along with the corresponding results.

1.1. A Typical Measuring Sequence

A combination of STF & multi-turnover flash (MTF) bursts was used to close PSII reaction centres in dark-adapted samples. A typical STF burst comprised 250 pulses, each lasting 130 μs , with 3 ms intervals between pulses and an intensity of $60,000 \mu\text{mol m}^{-2} \text{s}^{-1}$ red excitation light unless mentioned otherwise. The MTF pulse was ≤ 1 ms long and had an intensity of $15,000 \mu\text{mol m}^{-2} \text{s}^{-1}$. A combination STF, MTF and actinic light were used to design NPQ kinetics experiments (Fig. 12).

FI' Curve:

The first FI' data point is recorded after the first STF pulse and the FI' curve is obtained by recording data points after each STF pulse in the burst sequence. The increase in fluorescence is due to the reduction of Q_A , marking the closure of PSII reaction centres. The highest FI' data point of the first curve (FI'(1)) represents the maximum fluorescence (F_m), reflecting the closure of all PSII reaction centres following the initial excitation.

FIR' Curve:

The first FIR' data point of the first curve (FIR'(1)) represents the minimum fluorescence (F_0), reflecting the state of PSII reaction centres before the first photochemical event. The FIR' curve is obtained by recording data points before each STF pulse in the burst sequence,

which reflects the decrease in PSII fluorescence following the previous excitation. This decrease in fluorescence indicates the extent to which the PSII reaction centres return to their open state after each turnover.

By recording both F_i' and F_{iR}' curves during STF bursts, these measurements can provide a comprehensive analysis of PSII dynamics across multiple turnovers.

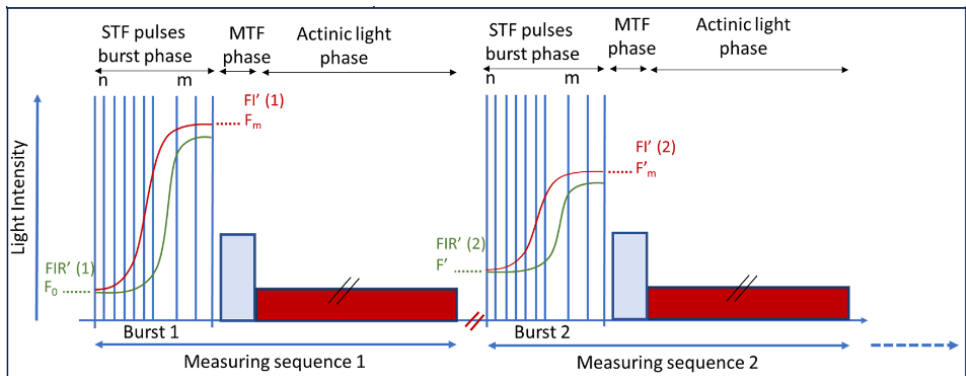


Fig. 12 Timing diagram of a typical measurement protocol. The sequence begins with a single turnover flash (STF) burst ($130 \mu\text{s}$ pulses of $60,000 \mu\text{mol m}^{-2} \text{s}^{-1}$) to determine F_0 and F_m from a dark-adapted leaf. This is followed by a short multi-turnover flash (MTF) and an actinic light phase. A second STF burst then measures F_i' and F_m at various wavelengths. The sequence can be repeated as required for experimental design. Source: Nanda *et al.*, 2024.

1.2. Wavelength-Dependent F_i' Curves and NPQ Measurements

Wavelength-dependent F_i' curves and NPQ measurements revealed variations in PSII efficiency and heterogeneity across different spectral regions respectively.

Wavelength-Dependent F_i' Curves:

F_i' curves for dark-adapted leaves of WT *Arabidopsis thaliana* were recorded using both the conventional PAM system and ChloroSpec. While PAM used only MTF pulses, ChloroSpec employed STF bursts followed by an MTF pulse. The STF-based method also captured the rapid rise in F_i' curves within the first 0.01 to 0.14 milliseconds of the measurements (Fig. 2, Paper I).

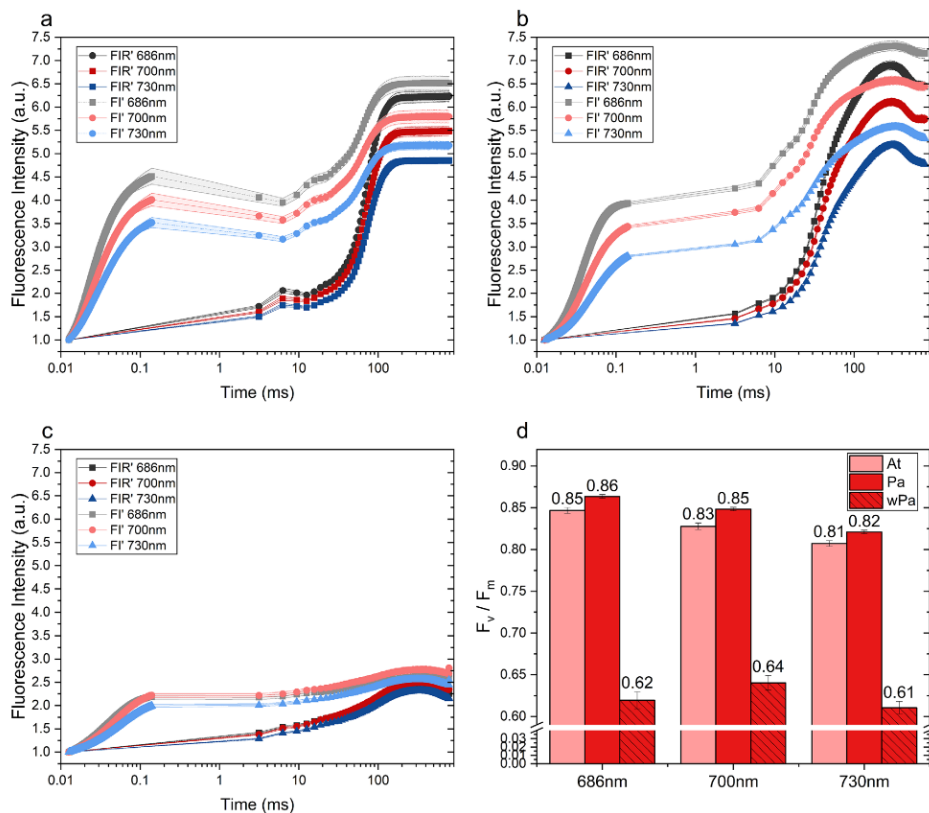


Fig. 13 Normalised fluorescence induction curves showing the evolution of FIR' and FI' during the first STF burst phase under red excitation light for (a) *A. thaliana* (At) leaves, (b) *P. abies* (Pa) needles, and (c) winter *P. abies* (wPa). (d) F_v/F_m values of At leaves and Pa needles measured at 686 nm, 700 nm, and 730 nm. Source: Nanda *et al.*, 2024.

Key observations from the wavelength-dependent FI' curves of WT *Arabidopsis thaliana* and *Picea abies* include:

- Plant species-specific differences were evident in the FI' curves. In *P. abies*, F'_m values declined towards the end phase of STF bursts, while in *A. thaliana*, it remained constant. This suggests faster PSII closure (highest value in the FI'(1) curve is defined as the F_m) in *P. abies*. Additionally, in winter *P. abies*, the FI lacks wavelength dependency and exhibits significantly reduced intensity due to the strongly quenched state (Fig. 13 a-c).

- The maximum quantum efficiency of PSII (F_v/F_m) was higher in the 680-700 nm range compared to 730 nm, with F_v/F_m values ranging from 0.61 to 0.86. Winter *Picea abies* exhibited low F_v/F_m compared to summer samples, demonstrating the impact of environmental conditions (Fig. 13d).

NPQ Measurements:

NPQ kinetics measurements were performed on WT *A. thaliana* and *P. abies* to investigate photoprotective mechanisms across different spectral regions. NPQ was induced in dark-adapted samples using actinic light. Fluorescence spectra were captured and analysed throughout the NPQ induction phase.

NPQ was significantly higher at 686 nm for both plant species, with *P. abies* displaying NPQ values between 2.5 and 5, and *A. thaliana* showing values between 1.5 and 2. (Fig. 14a).

- The FI' spectra during NPQ induction demonstrated clear shifts in fluorescence intensity and spectral characteristics over time (Fig. 14c-d). The NPQ spectra indicated that values peaked around 680-690 nm and were lower between 710-730 nm by the end of the actinic light phase, suggesting wavelength-specific differences in NPQ in both plant species (Fig. 14e-f).
- Growth conditions also played a significant role, with winter *P. abies* showing diminished NPQ at 686 nm compared to summer samples, underscoring how environmental factors influence NPQ behaviour (Fig. S4c, Nanda *et al.*, 2024).

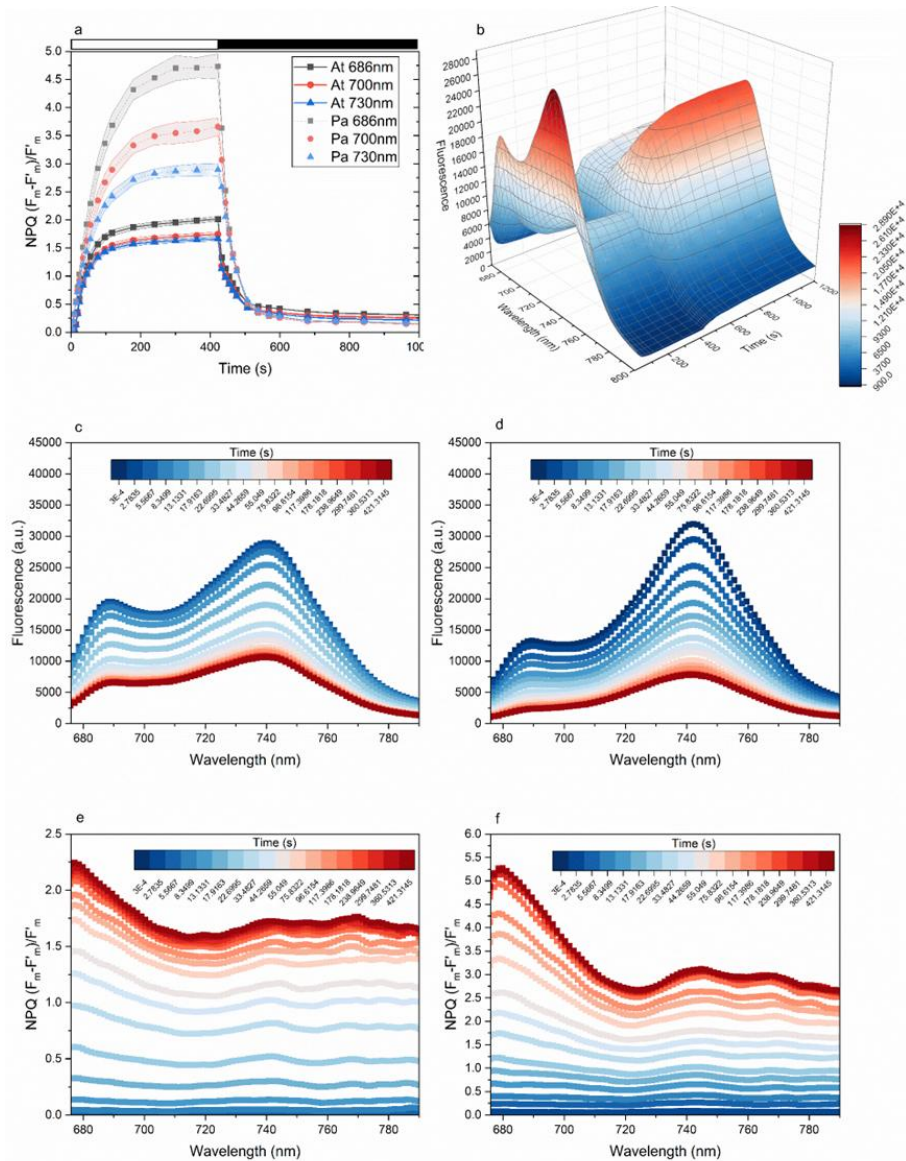


Fig. 14 (a) NPQ induction (white bars) and relaxation (dark bars) kinetics measured in *A. thaliana* (At) leaves and *P. abies* (Pa) summer needles at wavelengths of 686 nm, 700 nm, and 730 nm. NPQ was induced by $800 \mu\text{mol m}^{-2} \text{s}^{-1}$ red actinic light. Data are shown as means \pm SE ($n = 3$). (b) 3D spectra representation of fluorescence decrease (NPQ induction) and increase (NPQ relaxation) as a function of wavelength (670–800 nm) and time (s) for an At leaf. (c-d) 2D FI' spectra and (e-f) NPQ spectra for At and Pa during the actinic phase of NPQ kinetics, derived from the measurements in (a). Source: Nanda *et al.*, 2024.

1.3 Spectro-Kinetic Analysis of Chlorophyll Fluorescence Data

Steps Leading to the Best-Fit Model using Global Target Analysis

The $FI'(t,\lambda)$ surfaces (Fig. 14b) served as the foundation for applying global target analysis, allowing the resolution of temporal and spectral contributions that provide detailed insights into NPQ.

For *A. thaliana*, model refinement began with a two-component kinetic scheme, which resulted in a high χ^2 value (465.15, Fig. 15a). Additional components were sequentially incorporated, improving the fit and reducing χ^2 values (Fig. 15b). However, evaluating emission spectra and time-dependent concentration profiles (Fig. 15c) revealed that concentration of component 4 did not stabilize. A fifth component was added, but components 3 - 5 still failed to reach stable concentrations during the NPQ induction phase (Fig. 15d). To address this, a split reaction was introduced in component 2, yielding the final best-fit kinetic model for *A. thaliana* (Fig. 16a-b).

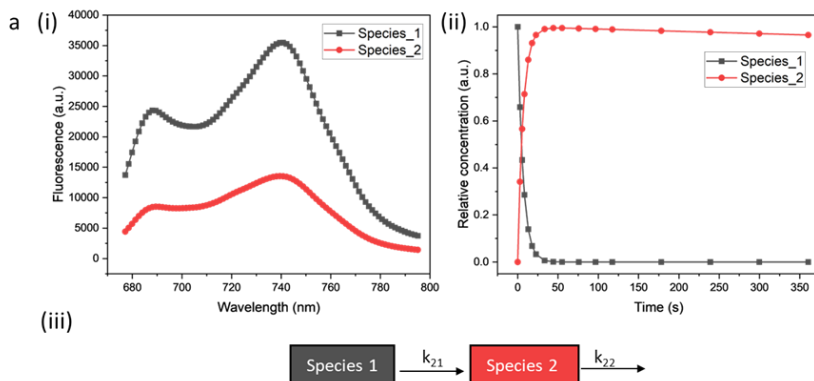


Fig. 15 Decomposition of NPQ fluorescence spectra global target analysis into (a) two components ($\chi^2 = 465.15$). NPQ induction kinetics data were obtained from an *A. thaliana* leaf exposed to $800 \mu\text{mol m}^{-2} \text{s}^{-1}$ red actinic light. (Continued on next page)

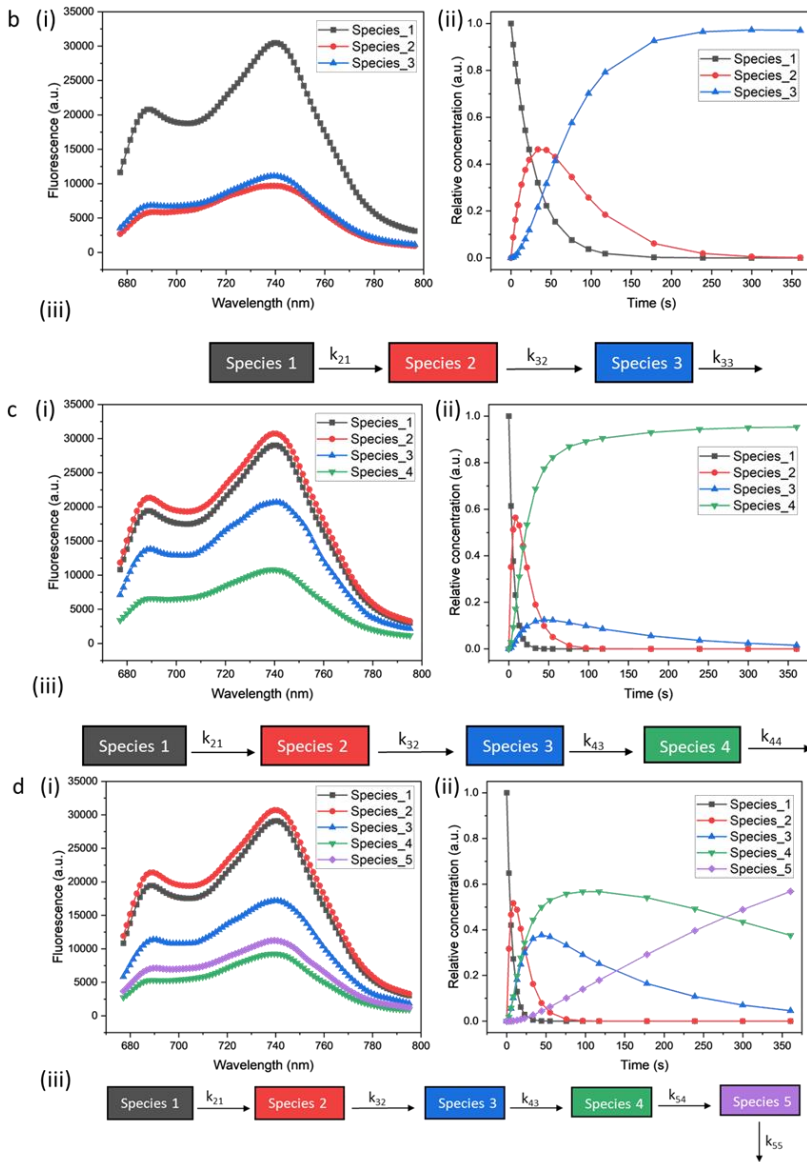


Fig. 15 (continued) Decomposition of NPQ fluorescence spectra global target analysis into (b) three components ($\chi^2 = 17.107$), (c) four components ($\chi^2 = 2.122$), and (d) five components ($\chi^2 = 1.959$). NPQ induction kinetics data were obtained from an *A. thaliana* leaf exposed to $800 \mu\text{mol m}^{-2} \text{s}^{-1}$ red actinic light. Source: Nanda *et al.*, 2024.

Comparison of Best-Fit Models in *A. thaliana* and *P. abies*

A five-component kinetic model was used for analysing both *A. thaliana* and *P. abies* with global target analysis (Fig. 16). The components derived from the kinetic model represent chlorophyll fluorescence species and will henceforth be referred to as 'species'. While the model framework is consistent, notable differences in spectral profiles and concentration dynamics reflect plant species-specific NPQ characteristics.

In *A. thaliana*, species 5, defined by a peak at 740 nm, exhibited the lowest fluorescence quantum yield, making it the most quenched component, whereas species 1 and 2 had the highest fluorescence yield (Fig. 16a). By the end of NPQ induction, species 3 and 5 reached stable concentrations, indicating their key roles in NPQ (Fig. 16b). Additionally, species 5 was present at a lower concentration than species 4 at this stage.

In *P. abies*, species 5 displayed a broader shoulder at 740 nm, more prominent than in *A. thaliana* (Fig. 16c) and reached a higher concentration than species 3 by the end of NPQ induction (Fig. 16d & f).

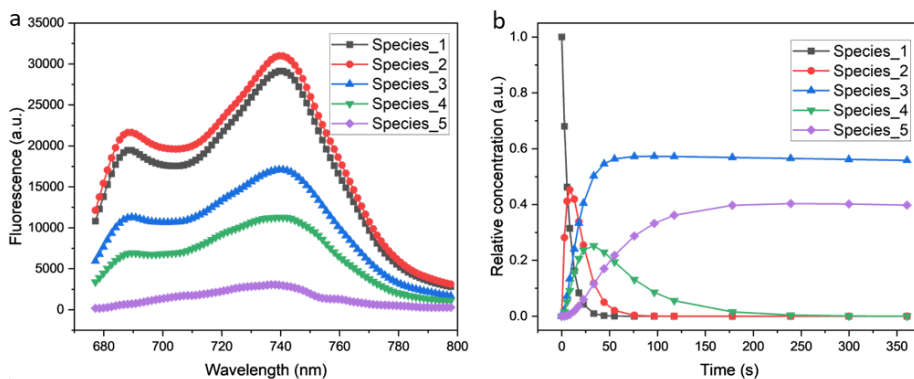


Fig. 16 Global target analysis results showing the decomposition of NPQ fluorescence data into five component spectra and their time-dependent concentration profiles are presented for (a)-(b) *A. thaliana* (total $\chi^2 = 1.76$). (Continued on next page)

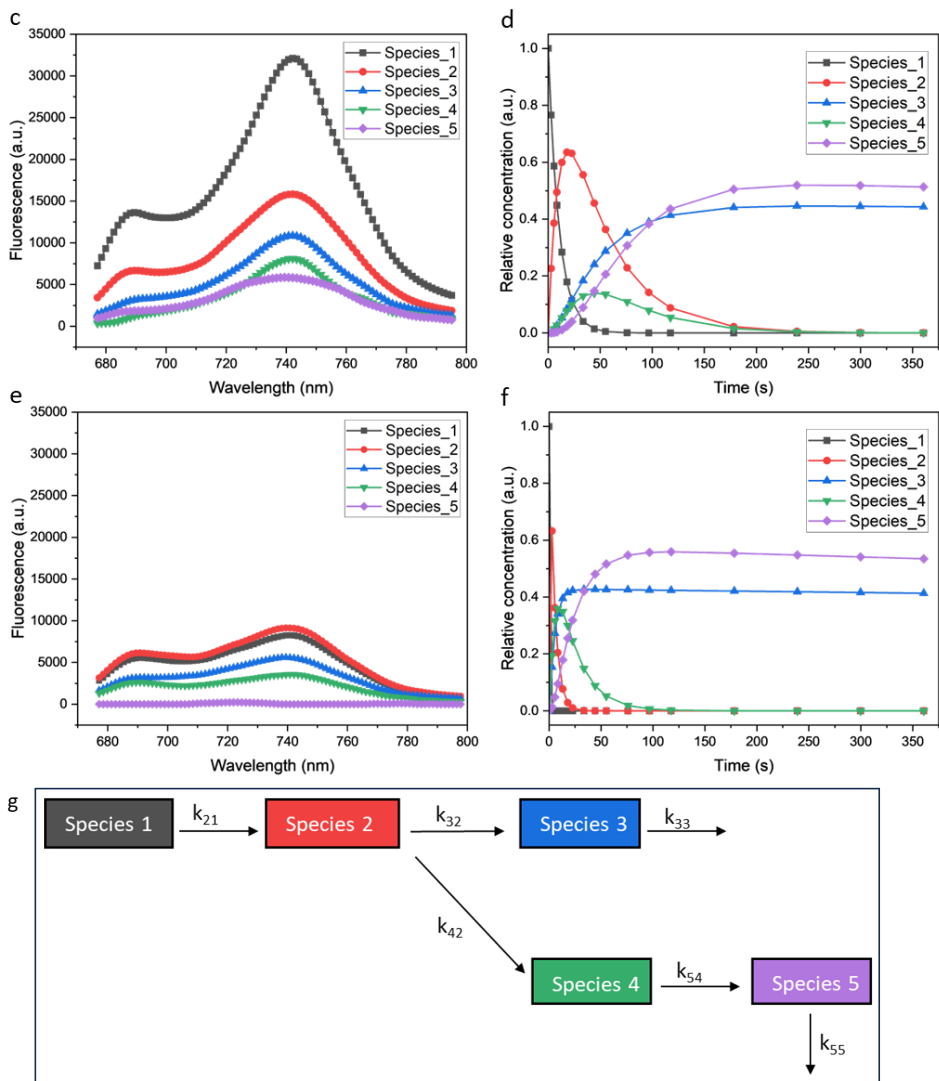


Fig. 16 (continued) (c)-(d) *P. abies* (total $\chi^2 = 1.97$) and (e)-(f) winter *P. abies* (total $\chi^2 = 0.15$). The corresponding kinetic scheme is illustrated in (g). NPQ induction kinetics were measured using $800 \mu\text{mol m}^{-2} \text{s}^{-1}$ red actinic light. Source: Nanda *et al.*, 2024.

Winter conditions in *P. abies* further altered NPQ dynamics, with decreased fluorescence intensity and distinctions between the five components becoming less pronounced. The characteristic broad shoulder of species 5 at 740 nm disappeared, reflecting stress-induced changes (Fig. 16e).

2. Insights into PSII and PSI contribution to NPQ: Spectroscopic Characterisation and its Correlation with Thylakoid Ultrastructure

This section presents the detailed results of MCR-ALS spectro-kinetic analysis conducted on *Arabidopsis*, hybrid aspen and pine, focusing on the identification of spectral components, concentration profiles, and their interpretations as detached LHCII quenching and PSII-PSI spillover components during NPQ induction. The analysis revealed five distinct entities and provides important insights into the roles of PsbS and zeaxanthin in regulating these processes. These findings expand our understanding of the mechanistic differences between plant species in their NPQ behaviour and the structural implications of light-induced changes in thylakoid organisation.

2.1. MCR-ALS Spectro-Kinetic Analysis of *Arabidopsis*, Aspen, and Pine

Spectral Components (Species)

Initial guesses for the species-associated emission spectra (SAES) in MCR-ALS analysis were obtained from global target analysis performed over a time range of ~120 seconds. The MCR-ALS analysis revealed five components/species and their associated emission spectra that satisfactorily describe the NPQ induction phase in WT *Arabidopsis*, hybrid aspen, and pine (Fig. 17). The normalised spectra (Fig. 17b, e & h) showed that species 1-3 were largely similar in shape. In contrast, species 4 and 5 showed significant increases in far-red fluorescence, particularly beyond 720 nm. While species 4 spectra is reminiscent of detached and quenched LHCII antennae, the species 5 spectra indicated a contribution from both PSII and PSI fluorescence, similar to the previously characterized PSII-PSI spillover observed in pine needles (Bag *et al.*, 2020). Species 5 was also identified as the most quenched species in all three plant species, reflecting its role as the dominant contributor to NPQ (Fig. 17 a, d, g).

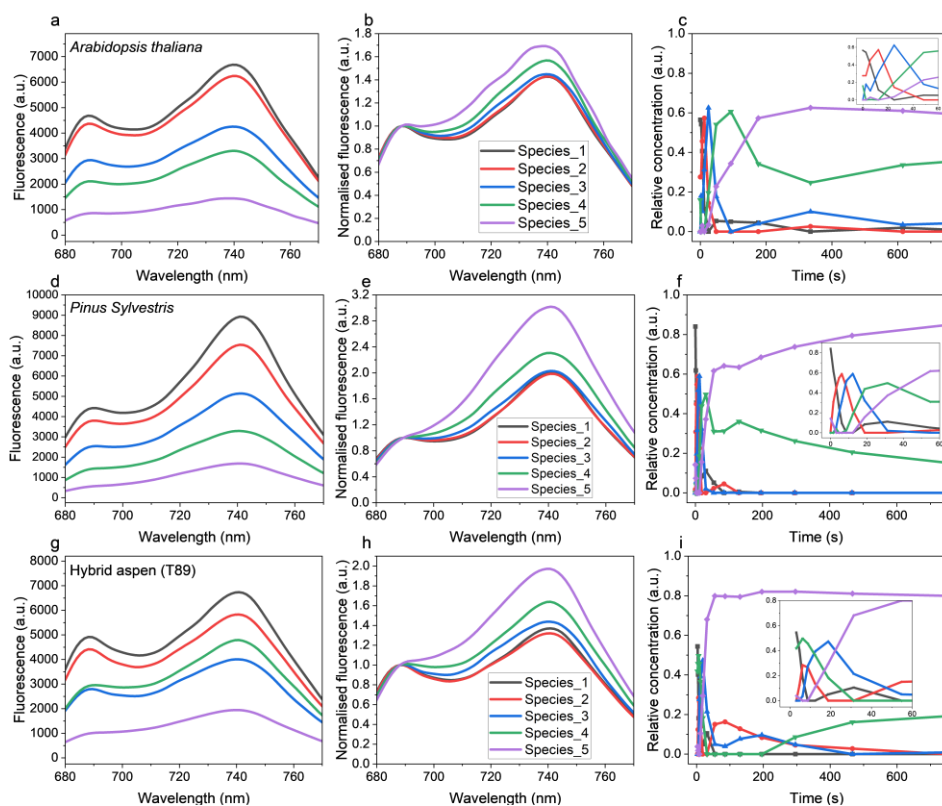


Fig. 17 Decomposition of the 3-dimensional fluorescence spectra during the NPQ induction phase was performed using MCR-ALS spectro-kinetic analysis, resulting in (a) species-associated emission spectra (SAES), (b) normalized SAES at 688 nm, and (c) time-dependent concentration profiles for WT *A. thaliana*. Similar analyses for WT *P. sylvestris* are presented in (d)–(f), and for WT hybrid aspen in (g)–(i). NPQ was induced in all samples using $600 \mu\text{mol m}^{-2} \text{s}^{-1}$ red actinic light. Source: Paper II.

Concentration Profiles and Quenching Dynamics

The concentration profiles of the five species provided insights into the sequence of biochemical reactions during NPQ induction. Species 1, representing the least quenched state, dominated the dark-adapted condition ($t = 0$), while species 2 and 3 emerged rapidly during the first 10–25 seconds of NPQ induction. Species 2 peaked around 10 seconds in *Arabidopsis* and subsequently decayed into species 3 and 4. Species 3 peaked at different times across the plant species (25 seconds in *Arabidopsis*, 15 seconds in pine, and 20 seconds in hybrid aspen),

indicating minor kinetic differences between plant species. Over time, species 4 and 5 began to dominate the long-term NPQ state, with species 5 contributing up to 80% of the absorption cross-section in hybrid aspen and pine and 60% in *Arabidopsis* (Fig. 17 c, f, i). The concentration profiles suggest that species 5 plays the central role in quenching during the NPQ phase, particularly in pine, which exhibited stronger spillover activity.

The quenching factor is a measure of how effectively a species dissipates excess energy as heat during NPQ. It is calculated by dividing the area under the curve of the unquenched species 1 by the area under the curve of the species in question. This ratio provides insight into the relative level of energy dissipation of each species. In this analysis, species 1, representing the dark-adapted, unquenched state, had the lowest quenching factor, while species 5 showed the highest quenching. The quenching factor for species 5 was determined to be 4.7, 3.7, and 5.4 for *Arabidopsis*, aspen, and pine, respectively (Table 1, Paper II).

A Scheme for NPQ

The scheme for NPQ development in plants describes a sequential reorganisation of photosynthetic complexes, transitioning through various biochemical states (Fig. 18). It begins with species 1, which represents the unquenched PSII supercomplex with minimal PSI fluorescence. This initial state transforms into species 2, characterised by the partial or full detachment of LHCII from PSII, while remaining unquenched. As species 2 diminishes, species 3 emerges, corresponding primarily to PSII cores. Over time, species 2 further decays, leading to the formation of two key quenched states: species 4, comprising detached and quenched LHCII, and species 5, representing the highly quenched PSII-PSI spillover phenomenon.

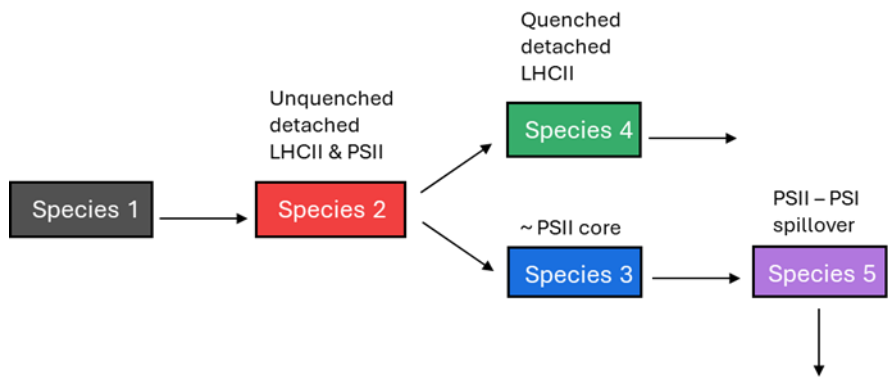


Fig. 18 A kinetic scheme for NPQ development derived from spectral characteristics and concentration profiles. The dominant species in the dark-adapted state is represented by Species 1, the intermediate and final states are depicted by the subsequent species as development of NPQ progresses over time. The respective species are represented using the same colour code used in Fig. 17. Source: Paper II.

2.2. Role of PsbS and Zeaxanthin

PsbS is required for the formation of detached & quenched LHCII

Arabidopsis npq4 mutants, which lack PsbS, exhibited significantly reduced NPQ (0.5-0.6) and a complete absence of the rapid, quenched LHCII detachment seen in WT plants (species 4). The absence of far-red contributions in the emission spectra of both *Arabidopsis npq4* and hybrid aspen *psbs* mutants confirmed that PsbS is essential for the formation of quenched and detached LHCII which in turn makes the PSII core available for PSII-PSI spillover (Fig. 19a-c and 20a-c). The MCR-ALS analysis revealed that only 3-4 species were needed to describe the NPQ kinetics in these mutants, compared to the 5 species in WT plants.

Arabidopsis L17 and the corresponding hybrid aspen oePsbS line, which demonstrated faster NPQ kinetics and enhanced quenching, particularly in species 5 (Fig. 19d-f and 20d-f). In hybrid aspen oePsbS, the quenching efficiency of species 5 was increased 3.6-fold compared to WT (Table 1, Paper II), indicating a significant enhancement of the spillover component. The faster kinetics observed in these lines, with all kinetic components 2-4 times faster than in WT, highlight the importance of PsbS in modulating the speed and efficiency of NPQ induction.

Zeaxanthin is required for efficient formation of PSII-PSI spillover

Arabidopsis npq1 mutants and the corresponding hybrid aspen *vde* mutants showed delayed NPQ kinetics and lacked the spillover component (Fig. 19g-i and 20g-i). The final NPQ state in *npq1* and *vde* mutants lacked a fully developed spillover complex, supporting the conclusion that zeaxanthin is required for efficient spillover formation during NPQ induction.

In contrast to the VDE mutants, *Arabidopsis npq2*, which accumulate high levels of zeaxanthin even in the dark, showed accelerated NPQ development. The *npq2* mutant followed a similar kinetic scheme as WT, but the formation of the spillover component occurred almost 10 times faster than in WT (Fig. 19j-l). The results suggest that the presence of high levels of zeaxanthin in *npq2* mutants allows for the rapid entry into the quenched state.

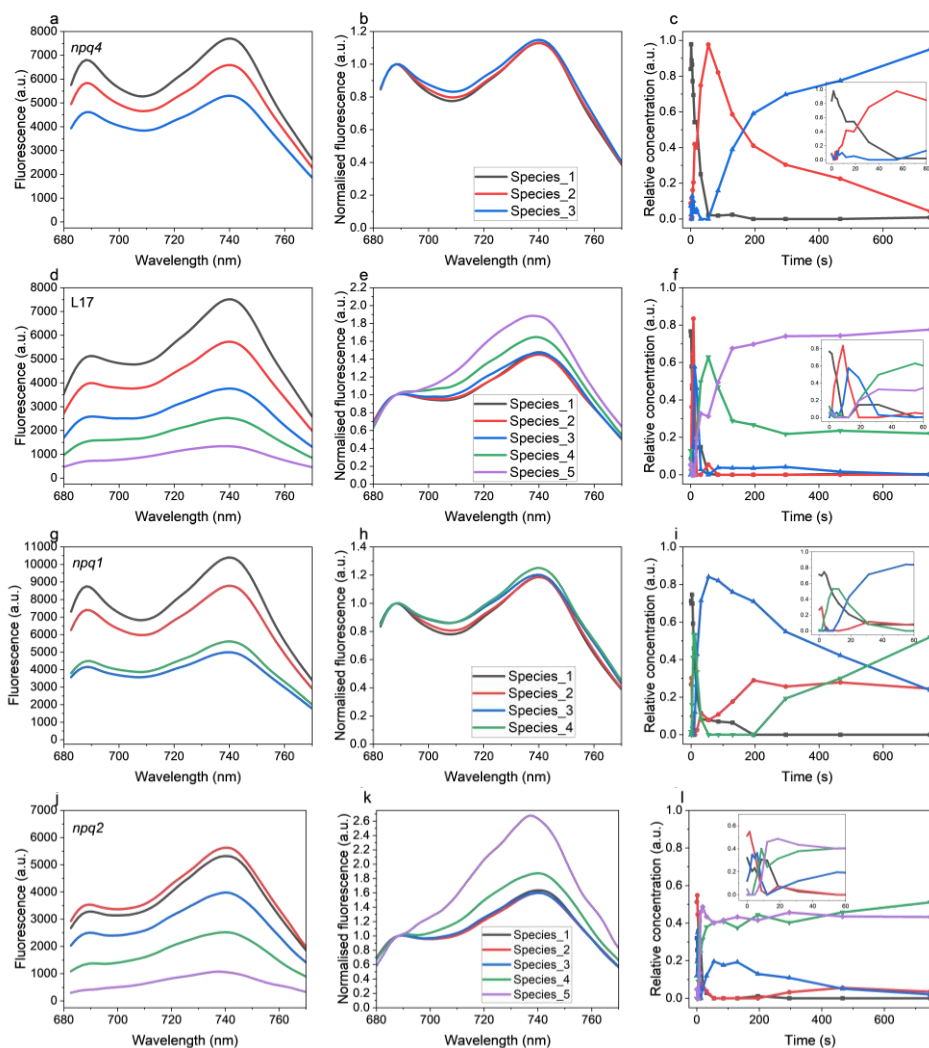


Fig. 19 Species-associated emission spectra (SAES), normalised SAES at 688 nm, and time-dependent concentration profiles for *Arabidopsis* genotypes were obtained by MCR spectro-kinetic analysis, respectively, for *npq4* (a, b, c); L17 (d, e, f); *npq1* (g, h, i) and *npq2* (j, k, l). Red actinic light at $600 \mu\text{mol m}^{-2} \text{s}^{-1}$ was used to induce NPQ in all samples. Source: Paper II.

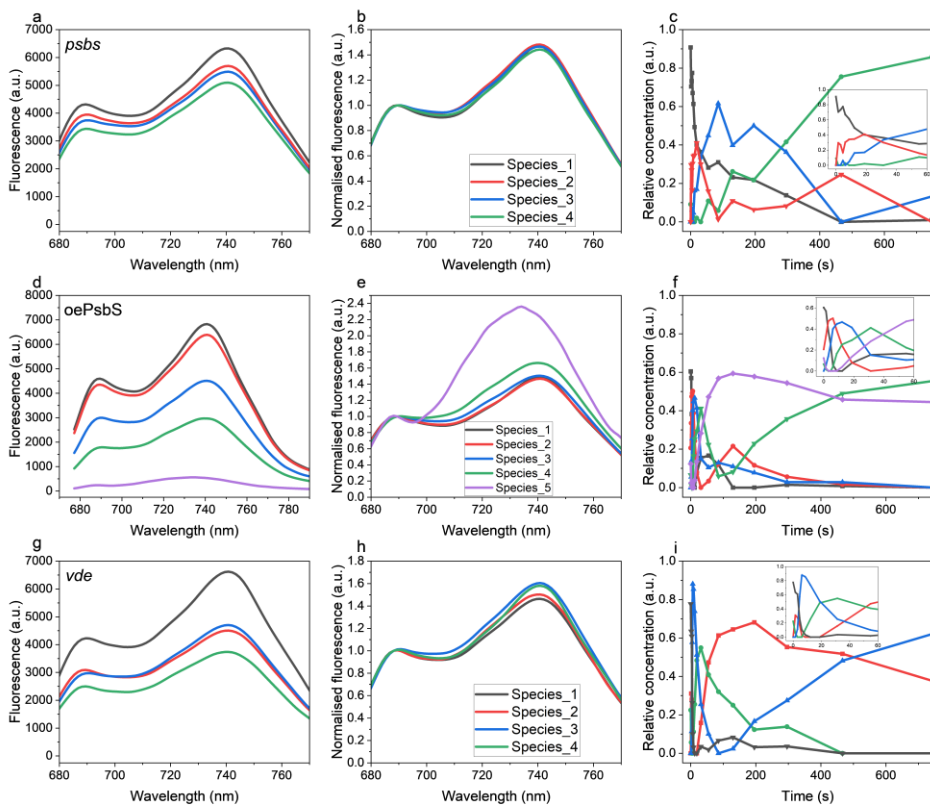


Fig. 20 Species-associated emission spectra (SAES), normalised SAES at 688 nm, and time-dependent concentration profiles for hybrid aspen lines were obtained by MCR spectro-kinetic analysis, respectively, for *psbs* (a, b, c); *oePsbS* (d, e, f) and *vde* (g, h, i). NPQ was induced in all samples using $600 \mu\text{mol m}^{-2} \text{s}^{-1}$ red actinic light. Source: Paper II.

2.3. Light-Induced Thylakoid Reorganisation and Its Impact on NPQ

To study the structural changes in thylakoid membranes during NPQ, TEM was performed on dark-adapted (D) and actinic light-adapted (AL) *Arabidopsis* leaves from various genotypes. A grana stack is defined as a structure with a minimum of two thylakoid layers stacked together.

Diameter of grana stacks are not severely affected by NPQ

The diameters represent the width of grana assuming the stacks are cylindrical in nature. There is an increase in diameter in *npq1* (9%) in NPQ state while no significant differences are observed in WT & *npq4* (Fig. 21). The frequency distribution of stack diameters show that most stacks are between 300-600 nm under both conditions with contrasting trends specifically in 300 nm and 600 nm stacks modulated by zeaxanthin (Fig. 22).

Grana destacking and increased stack numbers coincide with NPQ

The number of thylakoid layers per grana stack decreased under NPQ conditions (AL) in all examined genotypes except *npq2*, with WT plants showing a 24% reduction (Fig. 23a). The decrease was 18% in *npq1*, *npq4*, and 11% in L17, while *npq2* showed no significant changes in the number of layers per grana stack.

In contrast to the reduction in layers per grana stack, the number of grana stacks per chloroplast increased in WT and L17 plants under NPQ conditions (Fig. 23b). Wildtype showed a 40% increase in the number of grana stacks, while L17 plants exhibited an 11% increase. No significant changes in stack number were observed in *npq1*, *npq4*, or *npq2* mutants. The consistently high stack numbers in the mutant lines, observed in both dark and NPQ adapted states, suggest that the mutants have already elevated their stack formation in the dark as an adaptive response.

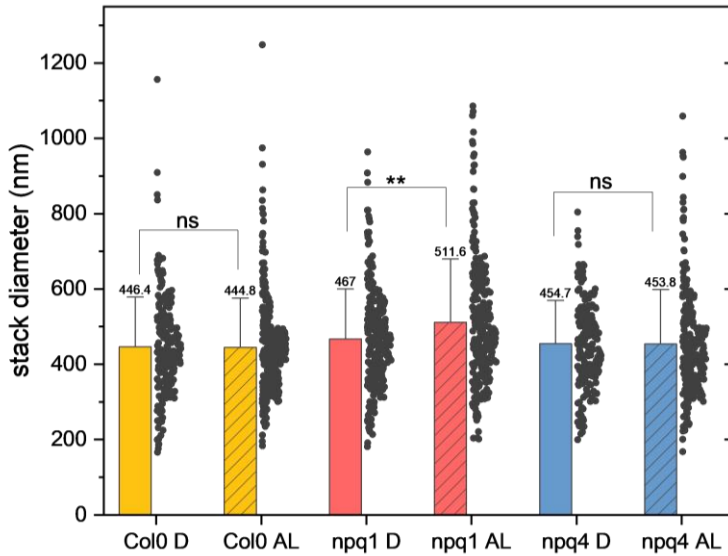


Fig. 21 Changes in stack diameter in Col-0 (WT), *npq1* & *npq4* upon actinic light induction. The diameter indicates the width of a grana based on the assumption that the grana stacks are cylindrical. Error bars represent standard deviation and mean values are represented above error bars calculated from n= 223 (Col-0 D), 315 (Col-0 AL), (*npq1* D), 273 (*npq1* AL), 200 (*npq4* D), 241 (*npq4* AL) of grana stacks where D (solid bars) is dark-adapted and AL (striped bars) is actinic light-adapted. Mann-Whitney test results are shown to compare D and AL conditions for each genotype ("*" = $p < 0.05$, "ns" = $p \geq 0.05$).

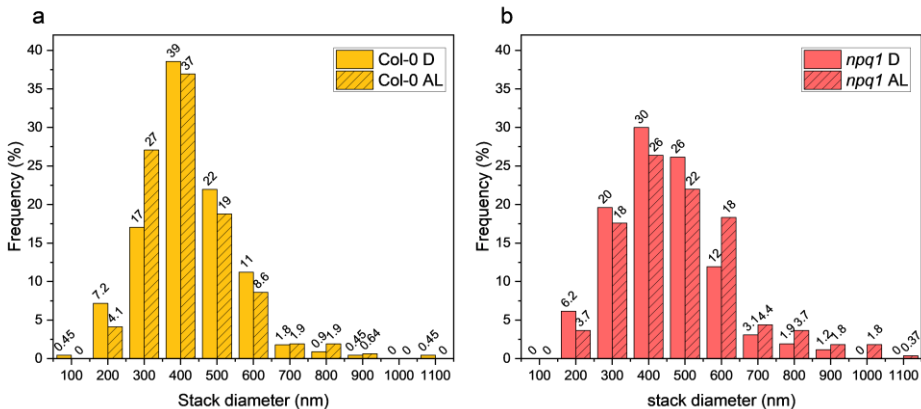


Fig. 22 Frequency distribution of grana stack diameter of (a) Col-0 (WT), (b) *npq1*. (Continued on next page)

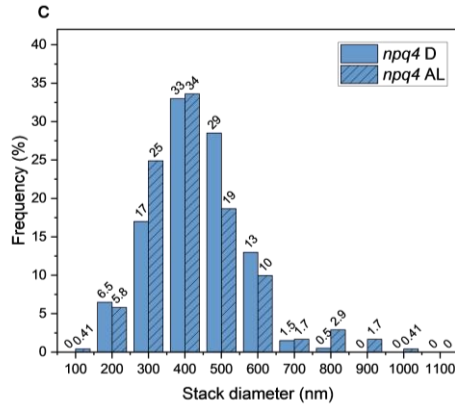


Fig. 22 (continued) (c) *npq4* in dark-adapted (D; solid bars) & actinic light-adapted (AL; striped bars) conditions as measured in Fig. 21. Percentage distributions are represented above each bar.

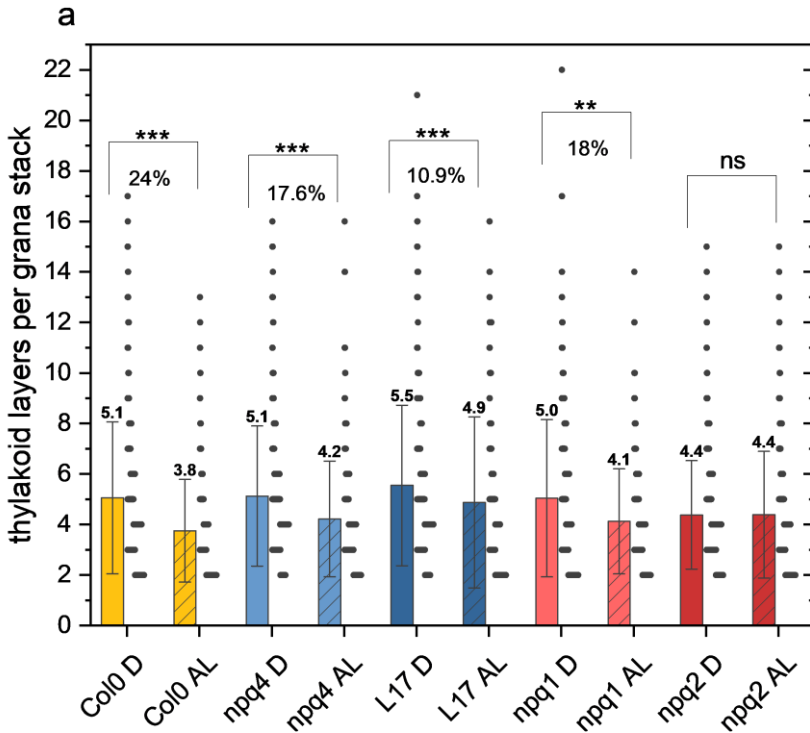


Fig. 23 Thylakoid reorganisation during NPQ induction was assessed as (a) the number of thylakoid layers per grana stack. (Continued on next page)

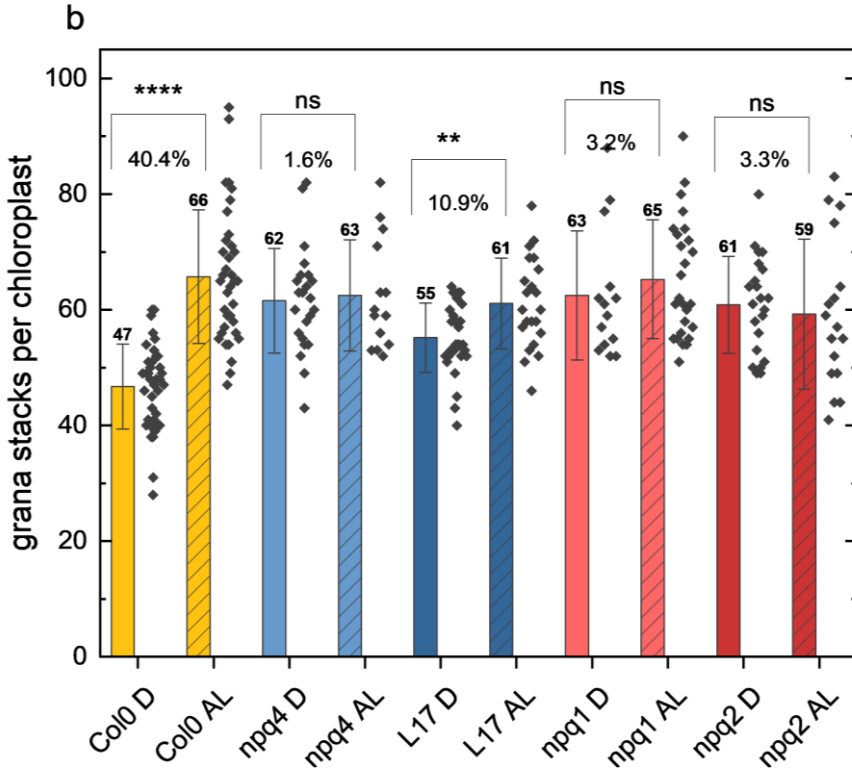


Fig. 23 (continued) (b) the number of grana stacks per chloroplast in *Arabidopsis* genotypes Col-0 (WT), *npq4*, L17, *npq1* and *npq2* under dark-adapted (D; solid bars) and actinic light-adapted (AL; striped bars) conditions. Mean values are displayed above the error bars, with standard deviation represented by error bars. Data for grana stacks in (a) were collected from n = 261 (Col-0 D), 268 (Col-0 AL), 276 (*npq1* D), 297 (*npq1* AL), 543 (*npq2* D), 296 (*npq2* AL), 255 (*npq4* D), 212 (*npq4* AL), 371 (L17 D), and 200 (L17 AL), while data for chloroplasts in (b) were collected from n = 38 (Col-0 D), 36 (Col-0 AL), 14 (*npq1* D), 26 (*npq1* AL), 22 (*npq2* D), 17 (*npq2* AL), 23 (*npq4* D), 14 (*npq4* AL), 31 (L17 D), and 22 (L17 AL). Mann-Whitney test results are shown to compare D and AL conditions for each genotype ("*" = $p < 0.05$, "ns" = $p \geq 0.05$), with percentage changes from D to AL displayed below the test results. Source: Paper II.

NPQ favors two-layered grana stacks modulated by zeaxanthin

Frequency distribution analysis of thylakoid layers per grana stack revealed additional insights into the impact of NPQ induction on thylakoid reorganization. The data revealed a clear shift towards two-layered stacks upon NPQ induction in WT and L17 plants, with the proportion of two-layered stacks increasing from 20% to 35% and 11% to 29%, respectively (Fig. 24 a, c). The *npq2* and *npq4* mutants also showed an increase in two-layered stacks, though less pronounced than in the WT and L17 plants (Fig. 24 b, e). In contrast, the *npq1* mutant exhibited no significant change in the proportion of two-layered stacks (Fig. 24 d). Notably, in the *npq2* mutant, which accumulates excess zeaxanthin, the increase in two-layered stacks occurred at the expense of three- and four-layered stacks. These findings suggest that NPQ favors the formation of two-layered stacks, with zeaxanthin playing a key role in modulating this shift.

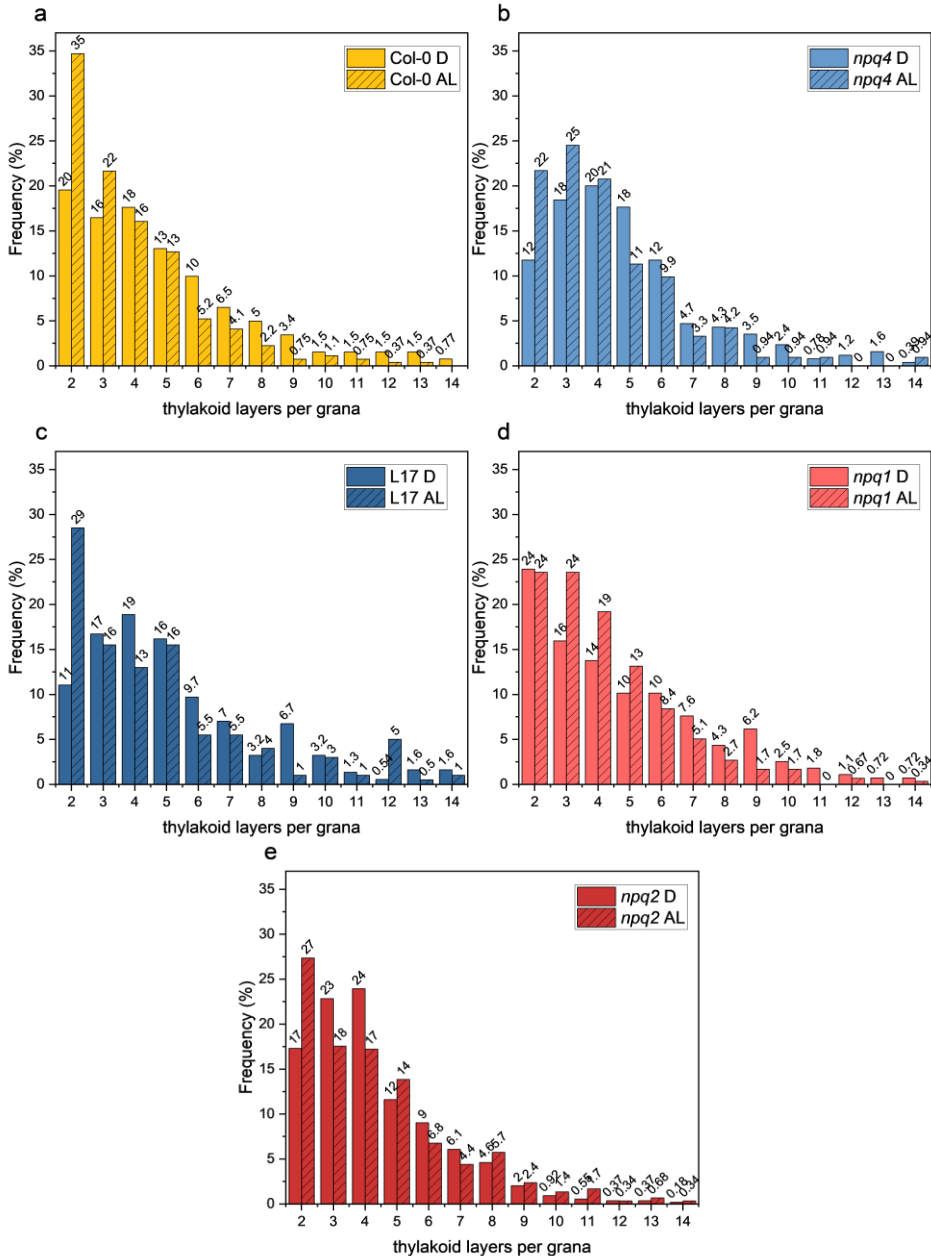


Fig. 24 The frequency distribution of thylakoid layers per grana stack in *Arabidopsis* (a) Col-0 (WT), (b) *npq4*, (c) L17, (d) *npq1* and *npq2* under dark-adapted (D, solid bars) and actinic light-adapted (AL, striped bars) conditions as measured in Fig. 23. Percentage distributions are indicated above each bar. Source: Paper II.

3. Exploring Photosynthetic Variation and Genetic Adaptations in Swedish Aspen

Chlorophyll fluorescence traits were measured from 97 genotypes from the SwAsp collection grown under controlled greenhouse conditions (Fig. 1, Paper III). While fluorescence traits like F_v/F_m exhibited minimal variation across genotypes, NPQ traits, including NPQ induction (NPQi) and NPQ relaxation (NPQr), showed substantial variability at 686 nm, 700 nm, and 730 nm (Figs. 3, S4, S5, Paper III). Strong correlations were observed between NPQ and fluorescence traits measured at different wavelengths (Fig. 25).

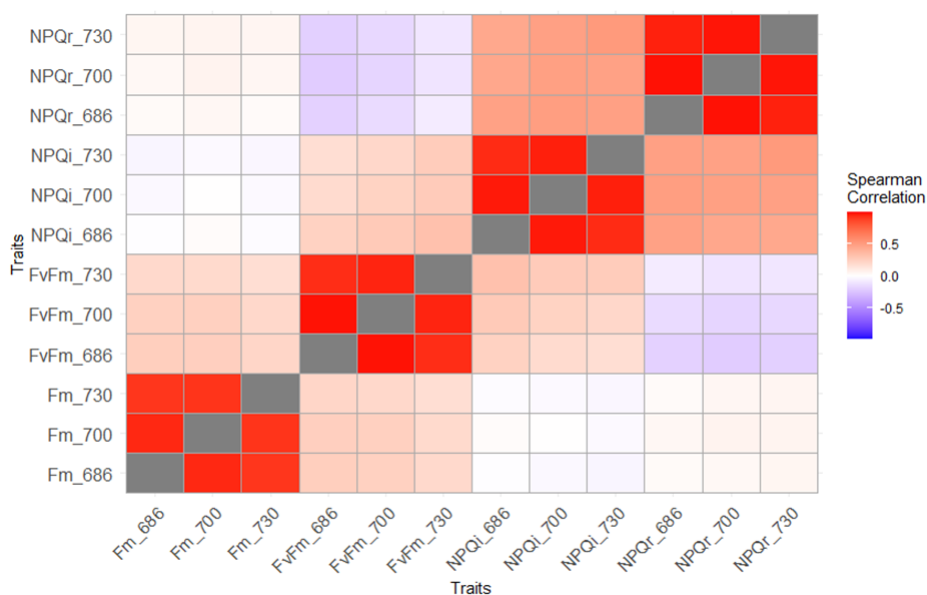


Fig. 25 The heatmap illustrates pairwise Spearman correlation coefficients (ρ) among the measured chlorophyll fluorescence traits, ranging from -1 (strong negative correlation, blue) to +1 (strong positive correlation, red). White spaces indicate non-significant correlations, while grey squares represent self-comparisons where each trait is compared to itself ($\rho=1$). Source: Paper III.

Analysis of the SwAsp population revealed no significant correlation between photosynthetic traits and latitude, with adjusted R^2 values below 0.1 for most traits (Fig. 5, Paper III). This suggests geographical origin had minimal impact on photosynthetic variation.

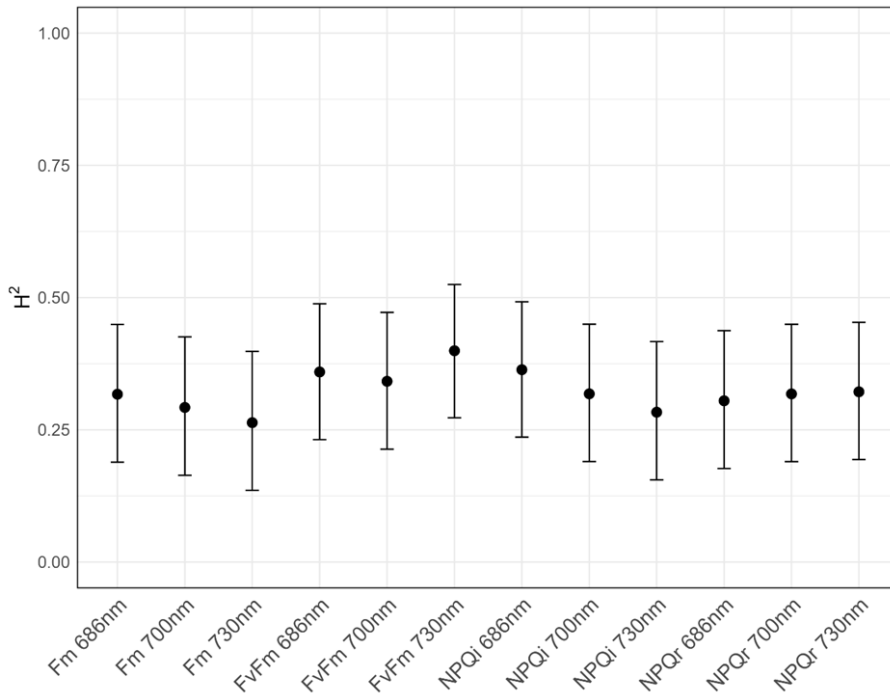


Fig. 26 The broad-sense heritability (H^2) of photosynthetic traits in the SwAsp population. The 95% confidence intervals are represented by the vertical bars. Source: Paper III.

Broad-sense heritability estimates for fluorescence traits were moderate (0.3–0.4) (Fig. 26). GWAS identified several single nucleotide polymorphisms (SNPs) significantly associated with F_m at 730 nm, including one near the *Lhca4* gene on Chr 15, a key component of PSI light-harvesting antennae (Fig. 27a). Individuals with the TT allele for this SNP showed higher F_m values than AA allele carriers, though overlapping distributions limit the biological relevance (Fig. 27b).

Co-expression analysis of *Lhca4* revealed a network of photosynthesis-related genes, with gene ontology (GO) enrichment highlighting processes linked to photosynthesis, thylakoid structure, and chlorophyll binding (Fig. 8, Paper III).

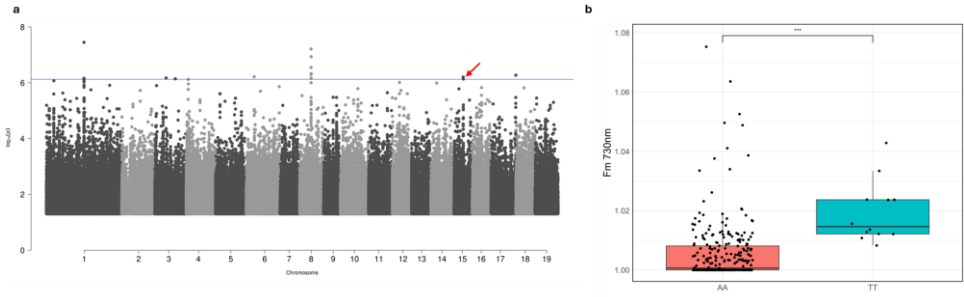


Fig. 27 Single nucleotide polymorphisms (SNPs) associated with the F_m trait at 730 nm are identified through genome-wide association analysis. (a) The Manhattan plot highlights the SNP linked to Potra2n15c28670 (Lhca4) with a red arrow, and the horizontal blue line marks a q-value threshold of 0.1. (b) A comparison of the F_m phenotype between homozygous recessive (TT) and dominant (AA) individuals for the highlighted SNP in the Potra2n15c28670 gene reveals significant differences. Source: Paper III.

4. Uncovering Molecular Players of the qH Photoprotective Mechanism in *Arabidopsis thaliana*

This study describes a whole-genome sequencing (WGS) approach to identify genetic factors underlying the qH mechanism in *Arabidopsis thaliana* by analysing EMS-mutagenized *soq1 npq4* mutants. Mutants associated with altered NPQ phenotypes were categorized into three main classes. The “normal green, low NPQ and low F_v/F_m due to high F_0 ” class, represented by mutants No.36 and No.39, exhibited increased F_0 , reduced NPQ, and low F_v/F_m , indicative of impaired PSII core function or antenna detachment (Fig. 3, Paper IV). These phenotypes may be caused by mutations in genes involved in PSII assembly or in enzymes like LTO1 (lumen thiol oxidoreductase 1), which regulates LCNP activity via redox mechanisms. The “pale green, low NPQ and lower F_v/F_m ” class, represented by mutants No.37 and No.245, displayed pale green pigmentation, a higher chlorophyll a/b ratio, and decreased NPQ (Fig. 4, Paper IV). These traits point to deficiencies in PSII antenna assembly or chlorophyll metabolism, potentially linked to mutations in genes like *cao* (chlorophyll a oxygenase) or *gun4* or *5* (genome uncoupled 4 and 5), which affect chlorophyll biosynthesis. Conversely, the “pale green, high NPQ and normal F_v/F_m ” class, represented by mutants No.251 and No.73, showed enhanced NPQ despite reduced chlorophyll content (Fig. 5, Paper IV). This phenotype may arise from mutations in Lhcb proteins, potentially leading to compensatory increases in quenching sites. Altered chloroplast ultrastructure could also reorganize antenna complexes, promoting qH. These findings highlight the roles of PSII assembly, chlorophyll metabolism, and light-harvesting complexes in regulating qH.

Conclusions & Perspectives

This section details a dissection of conclusions and perspectives, aligned with the aims and objectives outlined at the start of the thesis.

1. Addressing the NPQ Mechanism

This thesis highlights the pivotal roles of PsbS and zeaxanthin within a refined model of NPQ, emphasizing their contributions to energy dissipation. By employing advanced spectro-kinetic analysis alongside mutant studies, the findings illustrate how the fast initiation and efficient stabilisation of the spillover quenching state depend critically on these molecular components (Fig. 28a).

PsbS fulfils two key functions in NPQ. First, the presence of species 4 by MCR-ALS analysis captures a previously described LHCII quenching mechanism triggered by PsbS (Miloslavina *et al.*, 2008; Holzwarth *et al.*, 2009; Ostroumov *et al.*, 2020; Pawlak *et al.*, 2020). Additionally, PsbS plays an indirect role by facilitating spillover, which is characterized by energy transfer from PSII to PSI. The absence of PsbS significantly impairs both LHCII quenching and the development of the spillover component.

Zeaxanthin enhances NPQ efficiency by accelerating spillover formation. Its presence promotes the rapid transition from unquenched to strongly quenched states which is evident by the 10 times faster development of species 5 in *npq2* compared to WT (Fig. 19j-l). In the absence of zeaxanthin, the formation of species 3 is significantly delayed and we do not observe spillover in 10 minutes of NPQ induction (Fig. 19g-i). The role of zeaxanthin-induced spillover formation remains speculative. Zeaxanthin binding to Lhc proteins reduces triplet chlorophyll states in both PSII and PSI. In PSII, zeaxanthin interacts with monomeric Lhcb subunits like CP26 and CP24, while in PSI, it binds to Lhca3 and Lhca4, which host red-most chlorophyll forms acting as low-energy traps (Dall'Osto *et al.*, 2012). These traps, particularly in PSI, serve as deep-energy sinks, improving high-light tolerance by efficiently dissipating excess excitation energy (Yokono *et al.*, 2019). Together, these interactions position zeaxanthin as a critical regulator of spillover. The role of zeaxanthin in LHCII quenching is also a possibility since we do not observe the characteristic species 4 spectra in *npq1* and *vde*. Although models suggesting role of zeaxanthin in LHCII quenching have

been proposed (Wilk *et al.*, 2013; Sacharz *et al.*, 2017), LHCII isolated from *npq2* leaves only exhibits a slight quenching effect (with approximately 10-20% shorter lifetime, (Miloslavina *et al.*, 2008)), which is insufficient to explain the substantial *in vivo* NPQ effects observed. Another hypothesis is its indirect involvement via thylakoid reorganisation as discussed in the sub-section 3.

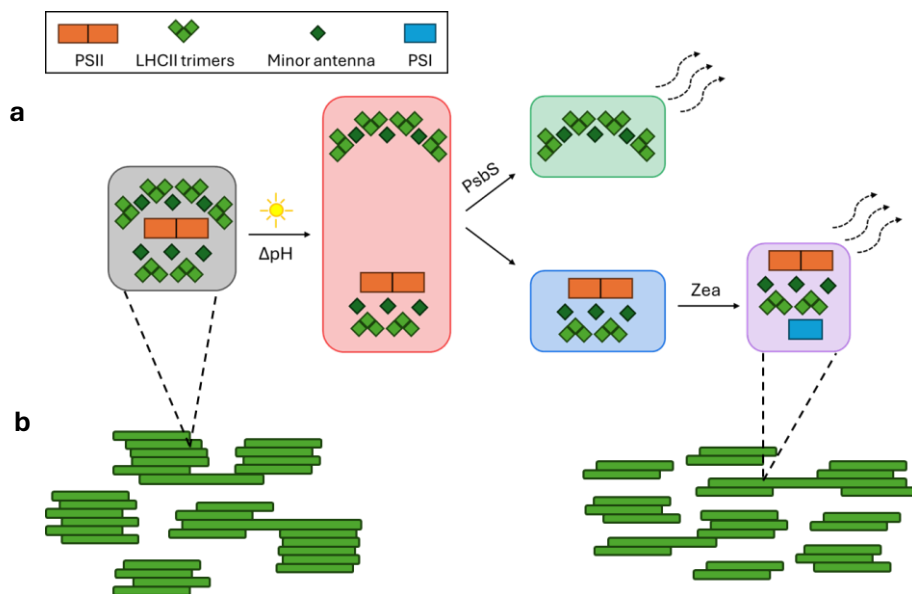


Fig. 28 Schematic representation of the proposed NPQ model in plants. (a) Biochemical processes during NPQ: The detachment of LHCII from the PSII core is triggered during the dark-to-light transition by lumen acidification (species 2). The detached LHCII fraction transitions rapidly into a quenched state (species 4) in presence of PsbS. The reduced absorption cross-section of PSII (species 3) interacts with PSI, forming the spillover megacomplex (species 5), facilitated by zeaxanthin. Each biochemical entity, enclosed in coloured boxes, corresponds to the spectral components deciphered in Fig. 18. Dashed arrows indicate energy dissipation by NPQ. (b) Changes in the thylakoid organisation: The dark-state grana (left side) feature highly stacked membranes. NPQ inducing light adaptation (right side) reorganizes the thylakoid structure, resulting in less stacking and a higher proportion of two-layered stacks, which increases the membrane surface for contact between PSI and PSII complexes. This structural shift facilitates spillover, and along with LHCII quenching triggered by PsbS, supports energy dissipation during NPQ.

2. Examining Functional Conservation of PsbS and Zeaxanthin in Angiosperms

In WT, aspen displayed faster NPQ kinetics, with the spillover component reaching half its peak concentration in 25 seconds compared to 100 seconds in *Arabidopsis* (Fig. 17c, i). Aspen also showed enhanced far-red characteristics in its normalized spectra, emphasizing superior spillover characteristics (Fig. 17h). Mutants lacking PsbS (*npq4* in *Arabidopsis*, *psbs* in aspen) exhibited reduced NPQ. Overexpression of PsbS enhanced NPQ in both species, though aspen relied more on detached LHCII quenching. Zeaxanthin-deficient mutants (*npq1* in *Arabidopsis*, *vde* in aspen) had no spillover formation. The comparative analysis of *Arabidopsis* and aspen reveals conserved roles for PsbS and zeaxanthin in driving photoprotective mechanisms but also highlights plant species-specific adaptations. Faster kinetics and pronounced spillover spectral features in hybrid aspen reflect its enhanced capacity for photoprotection.

3. Linking NPQ to Thylakoid Organisation

Thylakoid ultrastructural changes in response to light have been extensively documented. Notably, short-term adaptation (1 hour) from dark to light ($150 - 300 \mu\text{mol m}^{-2} \text{s}^{-1}$ white light) has been associated with an increase in the number of grana stacks per chloroplast in WT plants (Rozak *et al.*, 2002; Wood *et al.*, 2018, 2019). Concurrently, a decrease in the number of layers per grana stack under relatively higher growth light conditions ($500 \mu\text{mol m}^{-2} \text{s}^{-1}$ white light) has also been reported in WT (Flannery *et al.*, 2023). In this thesis, the thylakoid ultrastructure was specifically compared between two distinct states: dark-adapted (overnight adaptation) and NPQ adapted ($600 \mu\text{mol m}^{-2} \text{s}^{-1}$ red light for 30 minutes). Our findings complement previously reported data, suggesting that short-term adaptation under NPQ inducing actinic light also leads to thylakoid reorganisation.

The changes in thylakoid ultrastructure during NPQ induction underscore the intricate relationship between grana stacking and zeaxanthin. NPQ induction typically results in reduced grana stacking and a higher proportion of two-layered stacks. In the *npq2* mutant, the number of layers per grana stack was lower in the dark-adapted state (4.4 in *npq2* vs. 5.1 in WT), with no further reduction upon light exposure (Fig. 23a). Despite this, *npq2* exhibited an increase in two-layered stacks

at the expense of three- and four-layered stacks (Fig. 24). Conversely, *npq1* displayed no shift towards two-layered stacks, with reorganization favouring three- and four-layered stacks. Grana destacking leading to an increase in two-layered thylakoids may enhance the possibility for PSII-PSI spillover within grana end membranes and at grana margins. The formation of two-layered stacks increases the available surface area for spillover, potentially facilitating energy transfer between PSI in the grana end membranes and/or margins and PSII in adjacent appressed membranes (Fig. 28b).

In summary, our findings suggest that PsbS does not greatly influence thylakoid organisation, while zeaxanthin plays a significant role. These observations also underscore the complexity of thylakoid ultrastructure and highlight the substantial gaps in our understanding of its dynamics under diverse conditions.

4. Exploring Photosynthetic Variation in Aspen

This study explored natural variation in photosynthetic traits within a diverse population of *P. tremula* genotypes using the increased breadth of phenotyping by ChloroSpec. Significant variation in NPQ traits, with induction values varying almost two-fold among genotypes, underscores the potential for genetic analysis. NPQ along with F_v/F_m and F_m traits were effectively measured using a short protocol for understanding photosynthesis regulation. While a SNP near the *Lhca4* gene was associated with F_m at 730 nm, overlapping trait distributions suggest this association is likely a false positive. Although the study's population size limited statistical power, aspen remains a suitable model species. Future work should include larger populations and expanded phenotypic measurements to identify genetic regulators of photosynthetic traits.

Acknowledgements

As Forrest Gump's mother once wisely said, 'Life is like a box of chocolates; you never know what you're going to get.', my journey has certainly been no exception.

First and foremost, I extend my deepest gratitude to Stefan Jansson, my supervisor, for being the most positive person I have encountered and for always striving to make things work. Your open dialogue and unwavering encouragement have been a great source of inspiration, fostering both confidence and clarity. In moments when I felt like a stray photon, you helped me find direction and resonance. This journey has been both fulfilling and meaningful because of your support. I owe my chance at a PhD to you, Johannes Hanson, and Anita Sellstedt - your belief in me has been transformative.

My second and perhaps most heartfelt gratitude goes to my parents, Chaitali Nanda and Satadal Nanda. Through every triumph and challenge, your unwavering support has been the anchor of my life. The values you nurtured in me, coupled with your motivation through thick and thin, have fuelled my ambition and grounded me with stability. Despite the distance that has separated us these past years, your presence in my life has been an unshakable foundation.

To my lab group members - Tatyana Shutova, Kathryn Robinson, Nazeer Fataftah, Jenna Lihavainen, Maximiliano Cainzos, Chen Hu, and Dolores Pissolato, thank you for creating a stimulating environment where thoughts could bounce freely. The greenhouse team at UPSC deserves special thanks for their meticulous care of our plants, enabling our research to thrive. I am also deeply grateful to Agnieszka Ziolkowska at UCEM for the incredible crash course in electron microscopy and imaging - your expertise has been invaluable.

I am fortunate to have shared this journey with incredible friends who have made it so much more special. Thank you, Kristina Benevides, Sara Rydman, Camilla Canovi, Varvara Dikaya and Nabila El Arbi, for being a part of my Nordic adventure and adding a personal touch to every moment. To Sonja Viljamaa, Tuuli Aro, Luis Cervela Cardona, Aarón Benítez, Sarah Nardeli, Vasiliki Zacharaki, Ruben Benstein, Thomas Dobrenel and Laxmi Mishra, your indispensable tips and kind words came at just the right times - I cannot thank you enough. Sarah

Lundgren, Ellen Svensson and Ronja Lindgren, thank you for immersing me in all things Swedish and expanding my horizons. Madhusree Mitra, Sonali Ranade and Adity Majee, your presence helped nourish my Bengali roots and all things close to home in a foreign land. Lastly, to my long-time friends - Akriti Rajput, Radhika Vashishta and Sahiti Pale - thank you for helping me find sanity in insane times.

To all who have been a part of this journey, know that your support, love, and encouragement have been as vital as the very experiments that shaped this thesis. Thank you.

References

- Akhtar, P. *et al.* (2024) 'Quantifying the Energy Spillover between Photosystems II and I in Cyanobacterial Thylakoid Membranes and Cells', *Plant and Cell Physiology*, 65(1), pp. 95–106. Available at: <https://doi.org/10.1093/pcp/pcad127>.
- Allen, J.F. *et al.* (1981) 'Chloroplast protein phosphorylation couples plastoquinone redox state to distribution of excitation energy between photosystems', *Nature*, 291(5810), pp. 25–29. Available at: <https://doi.org/10.1038/291025a0>.
- Allen, J.F. (2003) 'State Transitions--a Question of Balance', *Science*, 299(5612), pp. 1530–1532. Available at: <https://doi.org/10.1126/science.1082833>.
- Allen, J.F. *et al.* (2011) 'A structural phylogenetic map for chloroplast photosynthesis', *Trends in Plant Science*, 16(12), pp. 645–655. Available at: <https://doi.org/10.1016/j.tplants.2011.10.004>.
- Allen, J.F. and Forsberg, J. (2001) 'Molecular recognition in thylakoid structure and function', *Trends in Plant Science*, 6(7), pp. 317–326. Available at: [https://doi.org/10.1016/S1360-1385\(01\)02010-6](https://doi.org/10.1016/S1360-1385(01)02010-6).
- Amstutz, C.L. *et al.* (2020) 'An atypical short-chain dehydrogenase–reductase functions in the relaxation of photoprotective qH in Arabidopsis', *Nature Plants*, 6(2), pp. 154–166. Available at: <https://doi.org/10.1038/s41477-020-0591-9>.
- Amunts, A., Drory, O. and Nelson, N. (2007) 'The structure of a plant photosystem I supercomplex at 3.4 Å resolution', *Nature*, 447(7140), pp. 58–63. Available at: <https://doi.org/10.1038/nature05687>.
- Andersson, B. and Anderson, J.M. (1980) 'Lateral heterogeneity in the distribution of chlorophyll-protein complexes of the thylakoid membranes of spinach chloroplasts', *Biochimica et Biophysica Acta (BBA) - Bioenergetics*, 593(2), pp. 427–440. Available at: [https://doi.org/10.1016/0005-2728\(80\)90078-X](https://doi.org/10.1016/0005-2728(80)90078-X).
- Armbruster, U. *et al.* (2013) 'Arabidopsis CURVATURE THYLAKOID1 Proteins Modify Thylakoid Architecture by Inducing Membrane Curvature[W]', *The Plant Cell*, 25(7), pp. 2661–2678. Available at: <https://doi.org/10.1105/tpc.113.113118>.

Aro, E.-M., Virgin, I. and Andersson, B. (1993) 'Photoinhibition of Photosystem II. Inactivation, protein damage and turnover', *Biochimica et Biophysica Acta (BBA) - Bioenergetics*, 1143(2), pp. 113–134. Available at: [https://doi.org/10.1016/0005-2728\(93\)90134-2](https://doi.org/10.1016/0005-2728(93)90134-2).

Aspinall-O'Dea, M. *et al.* (2002) 'In vitro reconstitution of the activated zeaxanthin state associated with energy dissipation in plants', *Proceedings of the National Academy of Sciences*, 99(25), pp. 16331–16335. Available at: <https://doi.org/10.1073/pnas.252500999>.

Atwell, S. *et al.* (2010) 'Genome-wide association study of 107 phenotypes in *Arabidopsis thaliana* inbred lines', *Nature*, 465(7298), pp. 627–631. Available at: <https://doi.org/10.1038/nature08800>.

Bag, P. *et al.* (2020) 'Direct energy transfer from photosystem II to photosystem I confers winter sustainability in Scots Pine', *Nature Communications*, 11(1), p. 6388. Available at: <https://doi.org/10.1038/s41467-020-20137-9>.

Baker, N.R. (1996) 'Photoinhibition of Photosynthesis', in R.C. Jennings *et al.* (eds) *Light as an Energy Source and Information Carrier in Plant Physiology*. Boston, MA: Springer US (NATO ASI Series), pp. 89–97. Available at: https://doi.org/10.1007/978-1-4613-0409-8_7.

Bellaïf, S. *et al.* (2005) 'State transitions and light adaptation require chloroplast thylakoid protein kinase STN7', *Nature*, 433(7028), pp. 892–895. Available at: <https://doi.org/10.1038/nature03286>.

van Bezouwen, L.S. *et al.* (2017) 'Subunit and chlorophyll organization of the plant photosystem II supercomplex', *Nature Plants*, 3(7), pp. 1–11. Available at: <https://doi.org/10.1038/nplants.2017.80>.

Bonente, G. *et al.* (2008) 'Interactions between the Photosystem II Subunit PsbS and Xanthophylls Studied *in Vivo* and *in Vitro**, *Journal of Biological Chemistry*, 283(13), pp. 8434–8445. Available at: <https://doi.org/10.1074/jbc.M708291200>.

Brooks, M.D. *et al.* (2013) 'A thioredoxin-like/ β -propeller protein maintains the efficiency of light harvesting in *Arabidopsis*', *Proceedings of the National Academy of Sciences*, 110(29), pp. E2733–E2740. Available at: <https://doi.org/10.1073/pnas.1305443110>.

Bru, P. *et al.* (2022) 'The major trimeric antenna complexes serve as a site for qH-energy dissipation in plants', *Journal of Biological*

Chemistry, 298(11). Available at:
<https://doi.org/10.1016/j.jbc.2022.102519>.

Bru, P., Nanda, S. and Malnoë, A. (2020) 'A Genetic Screen to Identify New Molecular Players Involved in Photoprotection qH in *Arabidopsis thaliana*', *Plants*, 9(11), p. 1565. Available at:
<https://doi.org/10.3390/plants9111565>.

Cazzaniga, S. *et al.* (2013) 'Interaction between avoidance of photon absorption, excess energy dissipation and zeaxanthin synthesis against photooxidative stress in *Arabidopsis*', *The Plant Journal*, 76(4), pp. 568–579. Available at: <https://doi.org/10.1111/tpj.12314>.

Chukhutsina, V.U., Holzwarth, A.R. and Croce, R. (2019) 'Time-resolved fluorescence measurements on leaves: principles and recent developments', *Photosynthesis Research*, 140(3), pp. 355–369. Available at: <https://doi.org/10.1007/s11120-018-0607-8>.

Croce, R. and van Amerongen, H. (2020) 'Light harvesting in oxygenic photosynthesis: Structural biology meets spectroscopy', *Science (New York, N.Y.)*, 369(6506). Available at:
<https://doi.org/10.1126/science.aay2058>.

Crouchman, S., Ruban, A. and Horton, P. (2006) 'PsbS enhances nonphotochemical fluorescence quenching in the absence of zeaxanthin', *FEBS Letters*, 580(8), pp. 2053–2058. Available at:
<https://doi.org/10.1016/j.febslet.2006.03.005>.

Dall'Osto, L. *et al.* (2012) 'Zeaxanthin Protects Plant Photosynthesis by Modulating Chlorophyll Triplet Yield in Specific Light-harvesting Antenna Subunits*', *Journal of Biological Chemistry*, 287(50), pp. 41820–41834. Available at: <https://doi.org/10.1074/jbc.M112.405498>.

Dall'Osto, L., Caffarri, S. and Bassi, R. (2005) 'A Mechanism of Nonphotochemical Energy Dissipation, Independent from PsbS, Revealed by a Conformational Change in the Antenna Protein CP26', *The Plant Cell*, 17(4), pp. 1217–1232. Available at:
<https://doi.org/10.1105/tpc.104.030601>.

De Souza, A.P. *et al.* (2022) 'Soybean photosynthesis and crop yield are improved by accelerating recovery from photoprotection', *Science*, 377(6608), pp. 851–854. Available at:
<https://doi.org/10.1126/science.adc9831>.

Demmig, B. *et al.* (1987) 'Photoinhibition and Zeaxanthin Formation in Intact Leaves 1 2: A Possible Role of the Xanthophyll Cycle in the Dissipation of Excess Light Energy', *Plant Physiology*, 84(2), pp. 218–224. Available at: <https://doi.org/10.1104/pp.84.2.218>.

Douady, D., Rousseau, B. and Berkaloff, C. (1993) 'Isolation and characterization of PSII core complexes from a brown alga, *Laminaria saccharina*', *FEBS Letters*, 324(1), pp. 22–26. Available at: [https://doi.org/10.1016/0014-5793\(93\)81524-4](https://doi.org/10.1016/0014-5793(93)81524-4).

Driever, S.M. *et al.* (2014) 'Natural variation in photosynthetic capacity, growth, and yield in 64 field-grown wheat genotypes', *Journal of Experimental Botany*, 65(17), pp. 4959–4973. Available at: <https://doi.org/10.1093/jxb/eru253>.

Fan, M. *et al.* (2015) 'Crystal structures of the PsbS protein essential for photoprotection in plants', *Nature Structural & Molecular Biology*, 22(9), pp. 729–735. Available at: <https://doi.org/10.1038/nsmb.3068>.

Faralli, M. and Lawson, T. (2020) 'Natural genetic variation in photosynthesis: an untapped resource to increase crop yield potential?', *The Plant Journal*, 101(3), pp. 518–528. Available at: <https://doi.org/10.1111/tpj.14568>.

Ferguson, J.N. *et al.* (2023) 'The genetic basis of dynamic non-photochemical quenching and photosystem II efficiency in fluctuating light reveals novel molecular targets for maize (*Zea mays*) improvement'. *bioRxiv*, p. 2023.11.01.565118. Available at: <https://doi.org/10.1101/2023.11.01.565118>.

Feyissa, B.A. *et al.* (2024) 'An orphan gene BOOSTER enhances photosynthetic efficiency and plant productivity', *Developmental Cell*, 0(0). Available at: <https://doi.org/10.1016/j.devcel.2024.11.002>.

Flannery, S.E. *et al.* (2023) 'STN7 is not essential for developmental acclimation of *Arabidopsis* to light intensity', *The Plant Journal*, 114(6), pp. 1458–1474. Available at: <https://doi.org/10.1111/tpj.16204>.

Flori, S. *et al.* (2017) 'Plastid thylakoid architecture optimizes photosynthesis in diatoms', *Nature Communications*, 8, p. 15885. Available at: <https://doi.org/10.1038/ncomms15885>.

Genty, B., Briantais, J.-M. and Baker, N.R. (1989) 'The relationship between the quantum yield of photosynthetic electron transport and quenching of chlorophyll fluorescence', *Biochimica et Biophysica Acta*

(*BBA*) - *General Subjects*, 990(1), pp. 87–92. Available at: [https://doi.org/10.1016/S0304-4165\(89\)80016-9](https://doi.org/10.1016/S0304-4165(89)80016-9).

Govindjee and Yang, L. (1966) 'Structure of the Red Fluorescence Band in Chloroplasts', *Journal of General Physiology*, 49(4), pp. 763–780. Available at: <https://doi.org/10.1085/jgp.49.4.763>.

Grimberg, Å. *et al.* (2018) 'Storage lipid accumulation is controlled by photoperiodic signal acting via regulators of growth cessation and dormancy in hybrid aspen', *New Phytologist*, 219(2), pp. 619–630. Available at: <https://doi.org/10.1111/nph.15197>.

Holzwarth, A.R. (1986) 'Fluorescence Lifetimes in Photosynthetic Systems', *Photochemistry and Photobiology*, 43(6), pp. 707–725. Available at: <https://doi.org/10.1111/j.1751-1097.1986.tb05650.x>.

Holzwarth, A.R. (1996) 'Data Analysis of Time-Resolved Measurements', in J. Amesz and A.J. Hoff (eds) *Biophysical Techniques in Photosynthesis*. Dordrecht: Springer Netherlands (Advances in Photosynthesis and Respiration), pp. 75–92.

Holzwarth, A.R. *et al.* (2009) 'Identification of two quenching sites active in the regulation of photosynthetic light-harvesting studied by time-resolved fluorescence', *Chemical Physics Letters*, 483(4), pp. 262–267. Available at: <https://doi.org/10.1016/j.cplett.2009.10.085>.

Holzwarth, A.R. and Jahns, P. (2014) 'Non-Photochemical Quenching Mechanisms in Intact Organisms as Derived from Ultrafast-Fluorescence Kinetic Studies', in B. Demmig-Adams *et al.* (eds) *Non-Photochemical Quenching and Energy Dissipation in Plants, Algae and Cyanobacteria*. Dordrecht: Springer Netherlands, pp. 129–156. Available at: https://doi.org/10.1007/978-94-017-9032-1_5.

Holzwarth, A.R., Wendler, J. and Haehnel, W. (1985) 'Time-resolved picosecond fluorescence spectra of the antenna chlorophylls in *Chlorella vulgaris*. Resolution of Photosystem I fluorescence', *Biochimica et Biophysica Acta (BBA) - Bioenergetics*, 807(2), pp. 155–167. Available at: [https://doi.org/10.1016/0005-2728\(85\)90119-7](https://doi.org/10.1016/0005-2728(85)90119-7).

Huang, X. *et al.* (2010) 'Genome-wide association studies of 14 agronomic traits in rice landraces', *Nature Genetics*, 42(11), pp. 961–967. Available at: <https://doi.org/10.1038/ng.695>.

Jansson, S. (1994) 'The light-harvesting chlorophyll ab-binding proteins', *Biochimica et Biophysica Acta (BBA) - Bioenergetics*, 1184(1), pp. 1–19. Available at: [https://doi.org/10.1016/0005-2728\(94\)90148-1](https://doi.org/10.1016/0005-2728(94)90148-1).

Jansson, S. (1999) 'A guide to the Lhc genes and their relatives in Arabidopsis', *Trends in Plant Science*, 4(6), pp. 236–240. Available at: [https://doi.org/10.1016/S1360-1385\(99\)01419-3](https://doi.org/10.1016/S1360-1385(99)01419-3).

Järvi, S. *et al.* (2011) 'Optimized native gel systems for separation of thylakoid protein complexes: novel super- and mega-complexes', *Biochemical Journal*, 439(2), pp. 207–214. Available at: <https://doi.org/10.1042/BJ20102155>.

Johnson, M.P. *et al.* (2011) 'Photoprotective Energy Dissipation Involves the Reorganization of Photosystem II Light-Harvesting Complexes in the Grana Membranes of Spinach Chloroplasts', *The Plant Cell*, 23(4), pp. 1468–1479. Available at: <https://doi.org/10.1105/tpc.110.081646>.

Johnson, M.P. and Ruban, A.V. (2010) 'Arabidopsis plants lacking PsbS protein possess photoprotective energy dissipation', *The Plant Journal*, 61(2), pp. 283–289. Available at: <https://doi.org/10.1111/j.1365-313X.2009.04051.x>.

Johnson, M.P. and Ruban, A.V. (2011) 'Restoration of Rapidly Reversible Photoprotective Energy Dissipation in the Absence of PsbS Protein by Enhanced ΔpH^* ', *Journal of Biological Chemistry*, 286(22), pp. 19973–19981. Available at: <https://doi.org/10.1074/jbc.M111.237255>.

Johnson, M.P. and Wientjes, E. (2020) 'The relevance of dynamic thylakoid organisation to photosynthetic regulation', *Biochimica et Biophysica Acta (BBA) - Bioenergetics*, 1861(4), p. 148039. Available at: <https://doi.org/10.1016/j.bbabi.2019.06.011>.

Kalaji, H.M. *et al.* (2014) 'Frequently asked questions about in vivo chlorophyll fluorescence: practical issues', *Photosynthesis Research*, 122(2), pp. 121–158. Available at: <https://doi.org/10.1007/s11120-014-0024-6>.

Kalaji, H.M. *et al.* (2017) 'Frequently asked questions about chlorophyll fluorescence, the sequel', *Photosynthesis Research*, 132(1), pp. 13–66. Available at: <https://doi.org/10.1007/s11120-016-0318-y>.

Kasahara, M. *et al.* (2002) 'Chloroplast avoidance movement reduces photodamage in plants', *Nature*, 420(6917), pp. 829–832. Available at: <https://doi.org/10.1038/nature01213>.

- Kautsky, H. and Hirsch, A. (1931) 'Neue Versuche zur Kohlensaureassimilation', *Die Naturwissenschaften*, 19(48), pp. 964–964. Available at: <https://doi.org/10.1007/BF01516164>.
- Kim, E. *et al.* (2023) 'Formation of a Stable PSI–PSII Megacomplex in Rice That Conducts Energy Spillover', *Plant and Cell Physiology*, 64(8), pp. 858–865. Available at: <https://doi.org/10.1093/pcp/pcado37>.
- Krause, G.H. (1988) 'Photoinhibition of photosynthesis. An evaluation of damaging and protective mechanisms', *Physiologia Plantarum*, 74(3), pp. 566–574. Available at: <https://doi.org/10.1111/j.1399-3054.1988.tb02020.x>.
- Krause, G.H. and Weis, E. (1991) 'Chlorophyll Fluorescence and Photosynthesis: The Basics', *Annual Review of Plant Biology*, 42(Volume 42, 1991), pp. 313–349. Available at: <https://doi.org/10.1146/annurev.pp.42.060191.001525>.
- Kromdijk, J. *et al.* (2016) 'Improving photosynthesis and crop productivity by accelerating recovery from photoprotection', *Science*, 354(6314), pp. 857–861. Available at: <https://doi.org/10.1126/science.aai8878>.
- Kumar, S. *et al.* (2018) 'MEGA X: Molecular Evolutionary Genetics Analysis across Computing Platforms', *Molecular Biology and Evolution*. Edited by F.U. Battistuzzi, 35(6), pp. 1547–1549. Available at: <https://doi.org/10.1093/molbev/msy096>.
- Küpper, H., Spiller, M. and Küpper, F.C. (2000) 'Photometric Method for the Quantification of Chlorophylls and Their Derivatives in Complex Mixtures: Fitting with Gauss-Peak Spectra', *Analytical Biochemistry*, 286(2), pp. 247–256. Available at: <https://doi.org/10.1006/abio.2000.4794>.
- Li, X.-P. *et al.* (2000) 'A pigment-binding protein essential for regulation of photosynthetic light harvesting', *Nature*, 403(6768), pp. 391–395. Available at: <https://doi.org/10.1038/35000131>.
- Lichtenthaler, H.K. (1992) 'The Kautsky effect: 60 years of chlorophyll fluorescence induction kinetics', *Photosynthetica*, 27(1–2), pp. 45–55.
- Lichtenthaler, H.K. and Buschmann, C. (2001) 'Chlorophylls and Carotenoids: Measurement UNIT F4.3 and Characterization by UV-VIS Spectroscopy', *Current Protocols in Food Analytical Chemistry*, F4.3.1-F4.3.8.

Madeira, F. *et al.* (2024) 'The EMBL-EBI Job Dispatcher sequence analysis tools framework in 2024', *Nucleic acids research*, 52(W1), pp. W521–W525. Available at: <https://doi.org/10.1093/nar/gkae241>.

Mähler, N. *et al.* (2020) 'Leaf shape in *Populus tremula* is a complex, omnigenic trait', *Ecology and Evolution*, 10(21), pp. 11922–11940. Available at: <https://doi.org/10.1002/ece3.6691>.

Malnoë, A. (2018) 'Photoinhibition or photoprotection of photosynthesis? Update on the (newly termed) sustained quenching component qH', *Environmental and Experimental Botany*, 154, pp. 123–133. Available at: <https://doi.org/10.1016/j.envexpbot.2018.05.005>.

Malnoë, A. *et al.* (2018) 'The Plastid Lipocalin LCNP Is Required for Sustained Photoprotective Energy Dissipation in *Arabidopsis*', *The Plant Cell*, 30(1), pp. 196–208. Available at: <https://doi.org/10.1105/tpc.17.00536>.

Mazor, Y., Borovikova, A. and Nelson, N. (2015) 'The structure of plant photosystem I super-complex at 2.8 Å resolution', *eLife*. Edited by W. Kühlbrandt, 4, p. e07433. Available at: <https://doi.org/10.7554/eLife.07433>.

Miloslavina, Y. *et al.* (2008) 'Far-red fluorescence: A direct spectroscopic marker for LHCII oligomer formation in non-photochemical quenching', *FEBS Letters*, 582(25), pp. 3625–3631. Available at: <https://doi.org/10.1016/j.febslet.2008.09.044>.

Müller, N.J.C. (1874) 'Beziehungen zwischen Assimilation, Absorption und Fluoreszenz im Chlorophyll des lebenden Blattes.', *Jahrbuch wiss Botanik*, (9), pp. 42–49.

Nanda, S. *et al.* (2024) 'ChloroSpec: A new in vivo chlorophyll fluorescence spectrometer for simultaneous wavelength- and time-resolved detection', *Physiologia Plantarum*, 176(2), p. e14306. Available at: <https://doi.org/10.1111/pp1.14306>.

Nawrocki, W.J. *et al.* (2016) 'State transitions redistribute rather than dissipate energy between the two photosystems in *Chlamydomonas*', *Nature Plants*, 2(4), pp. 1–7. Available at: <https://doi.org/10.1038/nplants.2016.31>.

Nawrocki, W.J. *et al.* (2021) 'Molecular origins of induction and loss of photoinhibition-related energy dissipation qI', *Science Advances*, 7(52), p. eabj0055. Available at: <https://doi.org/10.1126/sciadv.abj0055>.

Nilkens, M. *et al.* (2010) 'Identification of a slowly inducible zeaxanthin-dependent component of non-photochemical quenching of chlorophyll fluorescence generated under steady-state conditions in Arabidopsis', *Biochimica Et Biophysica Acta*, 1797(4), pp. 466–475. Available at: <https://doi.org/10.1016/j.bbabi.2010.01.001>.

Niyogi, K.K., Bjorkman, O. and Grossman, A.R. (1997) 'Chlamydomonas Xanthophyll Cycle Mutants Identified by Video Imaging of Chlorophyll Fluorescence Quenching.', *The Plant Cell*, 9(8), pp. 1369–1380. Available at: <https://doi.org/10.1105/tpc.9.8.1369>.

Niyogi, K.K., Grossman, A.R. and Björkman, O. (1998) 'Arabidopsis Mutants Define a Central Role for the Xanthophyll Cycle in the Regulation of Photosynthetic Energy Conversion', *The Plant Cell*, 10(7), pp. 1121–1134. Available at: <https://doi.org/10.2307/3870716>.

Ostroumov, E.E. *et al.* (2020) 'Characterization of fluorescent chlorophyll charge-transfer states as intermediates in the excited state quenching of light-harvesting complex II', *Photosynthesis Research*, 144(2), pp. 171–193. Available at: <https://doi.org/10.1007/s11120-020-00745-8>.

Patishtan, J. *et al.* (2018) 'Genome-wide association studies to identify rice salt-tolerance markers', *Plant, Cell & Environment*, 41(5), pp. 970–982. Available at: <https://doi.org/10.1111/pce.12975>.

Pawlak, K. *et al.* (2020) 'On the PsbS-induced quenching in the plant major light-harvesting complex LHCII studied in proteoliposomes', *Photosynthesis Research*, 144(2), pp. 195–208. Available at: <https://doi.org/10.1007/s11120-020-00740-z>.

Pfündel, E.E. (2021) 'Simultaneously measuring pulse-amplitude-modulated (PAM) chlorophyll fluorescence of leaves at wavelengths shorter and longer than 700 nm', *Photosynthesis Research*, 147(3), pp. 345–358. Available at: <https://doi.org/10.1007/s11120-021-00821-7>.

Pinnola, A. and Bassi, R. (2018) 'Molecular mechanisms involved in plant photoprotection', *Biochemical Society Transactions*, 46(2), pp. 467–482. Available at: <https://doi.org/10.1042/BST20170307>.

Pribil, M., Labs, M. and Leister, D. (2014) 'Structure and dynamics of thylakoids in land plants', *Journal of Experimental Botany*, 65(8), pp. 1955–1972. Available at: <https://doi.org/10.1093/jxb/eru090>.

Qin, X. *et al.* (2015) 'Structural basis for energy transfer pathways in the plant PSI-LHCI supercomplex', *Science*, 348(6238), pp. 989–995. Available at: <https://doi.org/10.1126/science.aab0214>.

Quick, W.P. and Stitt, M. (1989) 'An examination of factors contributing to non-photochemical quenching of chlorophyll fluorescence in barley leaves', *Biochimica et Biophysica Acta (BBA) - Bioenergetics*, 977(3), pp. 287–296. Available at: [https://doi.org/10.1016/S0005-2728\(89\)80082-9](https://doi.org/10.1016/S0005-2728(89)80082-9).

Rozak, P.R. *et al.* (2002) 'Rapid, reversible alterations in spinach thylakoid appression upon changes in light intensity', *Plant, Cell & Environment*, 25(3), pp. 421–429. Available at: <https://doi.org/10.1046/j.0016-8025.2001.00823.x>.

Ruban, A.V., Johnson, M.P. and Duffy, C.D.P. (2012) 'The photoprotective molecular switch in the photosystem II antenna', *Biochimica et Biophysica Acta (BBA) - Bioenergetics*, 1817(1), pp. 167–181. Available at: <https://doi.org/10.1016/j.bbabi.2011.04.007>.

Rungrat, T. *et al.* (2016) 'Using Phenomic Analysis of Photosynthetic Function for Abiotic Stress Response Gene Discovery', *The Arabidopsis Book*, 2016(14). Available at: <https://doi.org/10.1199/tab.0185>.

Rutan, S.C., de Juan, A. and Tauler, R. (2020) '2.06 - Introduction to Multivariate Curve Resolution☆', in S. Brown, R. Tauler, and B. Walczak (eds) *Comprehensive Chemometrics (Second Edition)*. Oxford: Elsevier, pp. 85–94. Available at: <https://doi.org/10.1016/B978-0-12-409547-2.14890-5>.

Sacharz, J. *et al.* (2017) 'The xanthophyll cycle affects reversible interactions between PsbS and light-harvesting complex II to control non-photochemical quenching', *Nature Plants*, 3(2), pp. 1–9. Available at: <https://doi.org/10.1038/nplants.2016.225>.

Satoh, K., Strasser, R. and Butler, W.L. (1976) 'A demonstration of energy transfer from photosystem II to photosystem I in chloroplasts', *Biochimica et Biophysica Acta (BBA) - Bioenergetics*, 440(2), pp. 337–345. Available at: [https://doi.org/10.1016/0005-2728\(76\)90068-2](https://doi.org/10.1016/0005-2728(76)90068-2).

Shapiguzov, A. *et al.* (2010) 'The PPH1 phosphatase is specifically involved in LHCI dephosphorylation and state transitions in Arabidopsis', *Proceedings of the National Academy of Sciences*, 107(10), pp. 4782–4787. Available at: <https://doi.org/10.1073/pnas.0913810107>.

Slavov, C. *et al.* (2016) “Super-quenching” state protects Symbiodinium from thermal stress – Implications for coral bleaching’, *Biochimica et Biophysica Acta (BBA) - Bioenergetics*, 1857(6), pp. 840–847. Available at: <https://doi.org/10.1016/j.bbabi.2016.02.002>.

Slavov, C., Reus, M. and Holzwarth, A.R. (2013) ‘Two Different Mechanisms Cooperate In The Desiccation-Induced Excited State Quenching In *Parmelia* Lichen’, *The Journal of Physical Chemistry B*, 117(38), pp. 11326–11336. Available at: <https://doi.org/10.1021/jp402881f>.

van Stokkum, I.H.M., Larsen, D.S. and van Grondelle, R. (2004) ‘Global and target analysis of time-resolved spectra’, *Biochimica et Biophysica Acta (BBA) - Bioenergetics*, 1657(2), pp. 82–104. Available at: <https://doi.org/10.1016/j.bbabi.2004.04.011>.

Strasser, R.J. and Govindjee (1992) ‘The Fo and the O-J-I-P Fluorescence Rise in Higher Plants and Algae’, in J.H. Argyroudi-Akoyunoglou (ed.) *Regulation of Chloroplast Biogenesis*. Boston, MA: Springer US, pp. 423–426. Available at: https://doi.org/10.1007/978-1-4615-3366-5_60.

Subhash, N. and Mohanan, C.N. (1997) ‘Curve-fit analysis of chlorophyll fluorescence spectra: Application to nutrient stress detection in sunflower’, *Remote Sensing of Environment*, 60(3), pp. 347–356. Available at: [https://doi.org/10.1016/S0034-4257\(96\)00217-9](https://doi.org/10.1016/S0034-4257(96)00217-9).

Sugiyama, K.-I. and Murata, N. (1978) ‘Analyses of absorption and fluorescence spectra of water-soluble chlorophyll proteins, pigment System II particles and chlorophyll *a* in diethylether solution by the curve-fitting method’, *Biochimica et Biophysica Acta (BBA) - Bioenergetics*, 503(1), pp. 107–119. Available at: [https://doi.org/10.1016/0005-2728\(78\)90165-2](https://doi.org/10.1016/0005-2728(78)90165-2).

Sundell, D. *et al.* (2015) ‘The Plant Genome Integrative Explorer Resource: PlantGenIE.org’, *New Phytologist*, 208(4), pp. 1149–1156. Available at: <https://doi.org/10.1111/nph.13557>.

Sylak-Glassman, E.J. *et al.* (2014) ‘Distinct roles of the photosystem II protein PsbS and zeaxanthin in the regulation of light harvesting in plants revealed by fluorescence lifetime snapshots’, *Proceedings of the National Academy of Sciences*, 111(49), pp. 17498–17503. Available at: <https://doi.org/10.1073/pnas.1418317111>.

Takahashi, S. and Murata, N. (2005) 'Interruption of the Calvin cycle inhibits the repair of Photosystem II from photodamage', *Biochimica et Biophysica Acta (BBA) - Bioenergetics*, 1708(3), pp. 352–361. Available at: <https://doi.org/10.1016/j.bbabi.2005.04.003>.

Terashima, I. *et al.* (2024) 'Excitation Spillover from PSII to PSI Measured in Leaves at 77K', *bioRxiv*, pp. 2024–04.

Tsai, Y.-C. *et al.* (2019) 'Chlorophyll fluorescence analysis in diverse rice varieties reveals the positive correlation between the seedlings salt tolerance and photosynthetic efficiency', *BMC Plant Biology*, 19(1), p. 403. Available at: <https://doi.org/10.1186/s12870-019-1983-8>.

Ünlü, C. *et al.* (2014) 'State transitions in *Chlamydomonas reinhardtii* strongly modulate the functional size of photosystem II but not of photosystem I', *Proceedings of the National Academy of Sciences*, 111(9), pp. 3460–3465. Available at: <https://doi.org/10.1073/pnas.1319164111>.

Wang, J. *et al.* (2018) 'A major locus controls local adaptation and adaptive life history variation in a perennial plant', *Genome Biology*, 19(1), p. 72. Available at: <https://doi.org/10.1186/s13059-018-1444-y>.

Wang, W. *et al.* (2023) 'Integration of high-throughput phenotyping, GWAS, and predictive models reveals the genetic architecture of plant height in maize', *Molecular Plant*, 16(2), pp. 354–373. Available at: <https://doi.org/10.1016/j.molp.2022.11.016>.

Ware, M.A., Belgio, E. and Ruban, A.V. (2015) 'Comparison of the protective effectiveness of NPQ in Arabidopsis plants deficient in PsbS protein and zeaxanthin', *Journal of Experimental Botany*, 66(5), pp. 1259–1270. Available at: <https://doi.org/10.1093/jxb/eru477>.

Weiss, C. (1972) 'The Pi electron structure and absorption spectra of chlorophylls in solution', *Journal of Molecular Spectroscopy*, 44(1), pp. 37–80. Available at: [https://doi.org/10.1016/0022-2852\(72\)90192-0](https://doi.org/10.1016/0022-2852(72)90192-0).

Welch, R. *et al.* (2021) 'Mechanisms shaping the synergism of zeaxanthin and PsbS in photoprotective energy dissipation in the photosynthetic apparatus of plants', *The Plant Journal*, 107(2), pp. 418–433. Available at: <https://doi.org/10.1111/tpj.15297>.

Wilk, L. *et al.* (2013) 'Direct interaction of the major light-harvesting complex II and PsbS in nonphotochemical quenching', *Proceedings of*

the National Academy of Sciences, 110(14), pp. 5452–5456. Available at: <https://doi.org/10.1073/pnas.1205561110>.

Wood, W.H.J. *et al.* (2018) ‘Dynamic thylakoid stacking regulates the balance between linear and cyclic photosynthetic electron transfer’, *Nature Plants*, 4(2), pp. 116–127. Available at: <https://doi.org/10.1038/s41477-017-0092-7>.

Wood, W.H.J. *et al.* (2019) ‘Dynamic Thylakoid Stacking Is Regulated by LHCII Phosphorylation but Not Its interaction with PSI’, *Plant Physiology*, 180(4), pp. 2152–2166. Available at: <https://doi.org/10.1104/pp.19.00503>.

Yokono, M. *et al.* (2019) ‘The PSI–PSII Megacomplex in Green Plants’, *Plant and Cell Physiology*, 60(5), pp. 1098–1108. Available at: <https://doi.org/10.1093/pcp/pcz026>.

Yokono, M., Murakami, A. and Akimoto, S. (2011) ‘Excitation energy transfer between photosystem II and photosystem I in red algae: Larger amounts of phycobilisome enhance spillover’, *Biochimica et Biophysica Acta (BBA) - Bioenergetics*, 1807(7), pp. 847–853. Available at: <https://doi.org/10.1016/j.bbabi.2011.03.014>.

Yokono, M., Noda, C. and Minagawa, J. (2024) ‘Spillover in the direct-type PSI-PSII megacomplex isolated from *Arabidopsis thaliana* is regulated by pH’, *Biochimica et Biophysica Acta (BBA) - Bioenergetics*, 1865(1), p. 149012. Available at: <https://doi.org/10.1016/j.bbabi.2023.149012>.